

Dynamic Factor Correlation Model*

Chen Tong[‡] and Peter Reinhard Hansen^{§†}

[‡]*Department of Finance, School of Economics, Xiamen University*

[§]*Department of Economics, University of North Carolina at Chapel Hill*

March 4, 2025

Abstract

We introduce a new dynamic factor correlation model with a novel variation-free parametrization of factor loadings. The model is applicable to high dimensions and can accommodate time-varying correlations, heterogeneous heavy-tailed distributions, and dependent idiosyncratic shocks, such as those observed in returns on stocks in the same subindustry. We apply the model to a “small universe” with 12 asset returns and to a “large universe” with 323 asset returns. The former facilitates a comprehensive empirical analysis and comparisons and the latter demonstrates the flexibility and scalability of the model.

Keywords: Factor Structure, Multivariate GARCH, Block Correlation Matrix, Heavy Tailed Distributions

JEL Classification: C32, C38, C55, C58

*The paper is based on results from the paper “Convolution- t distributions”, which was presented at the CIREQ-CMP Econometrics Conference in Honor of Eric Ghysels, Montreal, 2024.

[†]Corresponding author: Peter Reinhard Hansen. Email: hansen@unc.edu. Chen Tong acknowledges financial support from the Youth Fund of the National Natural Science Foundation of China (72301227), and the Ministry of Education of China, Humanities and Social Sciences Youth Fund (22YJC790117).

1 Introduction

In this paper, we propose a flexible factor-correlation model that can be scaled to high dimensions. The model relies on univariate volatility models to define the time series of standardized returns, $Z_{1,t}, \dots, Z_{n,t}$, and factor variable, $F_{1,t}, \dots, F_{r,t}$, and a multivariate GARCH model to capture the correlation structure among the factor variables, F_t . Our main contributions are the dynamic modeling of the factor loadings and the idiosyncratic correlation matrix with various structures. A key theoretical contribution is a variation-free parametrization of factor loading, which simplifies aspects of their modeling.

Univariate GARCH models have proven highly successful in capturing heteroscedasticity in individual return series since their introduction in Engle (1982) and the refinements in Bollerslev (1986). However, extending these models to the multivariate setting has been far less straightforward. A key challenge lies in preserving the positive definiteness of the covariance matrix in a natural and elegant manner. The number of covariance/correlation increases with the square of the dimension, and some structure is needed to make estimation feasible with high dimensional systems. Many multivariate GARCH formulations impose structure through parameter restrictions, that can be overly restrictive in their functional form, limiting their flexibility in capturing complex dependencies. This has led to a wide range of competing models, each addressing particular aspects of these challenges without providing a fully satisfactory generalization. Popular multivariate GARCH models, include the BEKK model¹ by Engle and Kroner (1995) and the Dynamic Conditional Correlation model by Engle (2002), which both have restrictive dynamic structures, especially in high dimensional setting.

Our paper relates to a very large body of literature including the studies on factor models. Factors are widely used in finance, and some use a *latent* factor structure, such as those by Oh and Patton (2017, 2018, 2023), Creal and Tsay (2015), and Opschoor et al. (2021) that use copula (latent) factor structure to model the dynamics of correlations, while assuming idiosyncratic shocks to be uncorrelated. Another strand of literature leverages *observed* factors, with some models relying on realized measures from high-frequency data to capture dynamic factor loadings. For instance, the Realized-Beta GARCH model of Hansen et al. (2014) is a one-factor model that utilizes realized correlations (between individual assets and the market return). They also document a strong dependence between idiosyncratic shocks, especially for stocks in the same sector. A related model is the Factor HEAVY model by Sheppard and Xu (2019), which also rely on realized measure (realized betas) for updating factor loadings. Other studies, such as Engle (2016) and Darolles et al. (2018), concentrate

¹BEKK is named after Baba, Engle, Kraft, and Kroner

on modeling time-varying betas without accounting for the idiosyncratic correlations.

The block correlation structure introduced by [Engle and Kelly \(2012\)](#) is a valuable contribution to the literature on multivariate volatility models, because it offers a parsimonious approach to modeling large-dimensional covariance matrices while preserving interpretability. The structure in [Engle and Kelly \(2012\)](#) does reduce the number of parameters, but it does not inherently guarantee positive semi-definiteness (PSD) and is cumbersome in situations with more than two blocks. This issue was later resolved by [Archakov and Hansen \(2024\)](#), who developed a method to ensure positive definite block correlation matrices for any number of blocks. This laid the foundation for the multivariate Realized GARCH model proposed by [Archakov et al. \(2025\)](#), which integrates realized measures of volatility within a coherent multivariate GARCH framework. In related work, [Tong et al. \(2024\)](#) introduced a score-driven multivariate GARCH model based on convolution- t distributions of [Hansen and Tong \(2024\)](#). This class of distributions has greater flexibility for capturing complex nonlinear dependencies, and can accommodate heterogeneous heavy-tailness and cluster structures in tail dependencies, which were limitations of traditional specifications with Gaussian and multivariate t -distributions.

In this paper, we will also adopt convolution- t distributions. However, our dynamic model of the correlation structure is entirely different from that in [Tong et al. \(2024\)](#). For instance, we include observable factors into the modeling and specify dynamic models for the corresponding factor loadings. Another key difference is that [Tong et al. \(2024\)](#) impose block structures on the correlation matrix for returns, whereas we impose block structures on the idiosyncratic correlation matrix, which enable us to adopt sparse block correlation matrices. The structure of the idiosyncratic correlation matrix plays a critical role in our modeling, and its sparse nature facilitates implementation in very high dimensions. Block correlation structures in idiosyncratic asset returns (related to industry sectors) is well documented in the empirical studies, including [Fan et al. \(2016\)](#), [Ait-Sahalia and Xiu \(2017\)](#), and [Andreou et al. \(2024\)](#), [Bodilsen \(2024\)](#), and [Hansen et al. \(2014\)](#). Most of the earlier literature involving dynamic factor models assume idiosyncratic asset returns to be uncorrelated.

We largely rely on the existing literature to model the univariate return series, as well as the dynamic correlation structure of factor variables. The contributions of this paper is mainly relates to the part of the model named the *Core Correlation Model*. This part has dynamic factor loadings and dynamic idiosyncratic correlation matrix, and it has a structure that makes it scalable to high dimensions. A key component in this part of the model is a novel variation-free parametrization of the dynamic factor loadings, which is inspired by the generalized Fisher transformation (GFT) of correlation matrices by [Archakov and Hansen \(2021\)](#). We rely heavily on the score driven framework by [Creal et al. \(2011\)](#) to specify

dynamic models of factor loadings and various correlation matrices, and in this context we utilize Tikhonov regularized Moore-Penrose inverse to ensure stable updating in the score-driven model. We draw heavily on Archakov and Hansen (2024) to formulate block correlation matrices and sparse versions of these. Importantly, the model is scalable to high dimensions, owing in part to a decoupled estimation method of the core correlation model.

We apply the new model to 17 years of daily stock returns. A *small universe* with $n = 12$ assets and a *large universe* with $n = 323$ assets. The small universe facilitates model comparisons under different specifications and estimation methods, which is not possible in high dimension, such as that of the large universe. As factor variables we adopt the six cross-sectional factors, known as the Fama-French five factors (FF5) and the momentum factor, and we include sector-specific factors that are based on exchange traded funds (ETFs) for each of the sectors. A sample correlation matrix motivates the use of subindustries to define the block structure in the idiosyncratic correlation matrix.

The empirical results are very encouraging. Applying the model to the large universe with $n = 323$ stocks and 63 subindustries poses no obstacles with decoupled estimation. We find strong empirical support for the specifications with convolution- t distributions that outperform the conventional multivariate t -distribution (and the Gaussian). This is true for both the small universe and the large universe, and holds in-sample as well as out-of-sample. The out-of-sample comparisons favors a sparse block correlation structure, but also shows that aside from correlations within subindustries there are often non-trivial correlations between stocks in different subindustries, but predominantly for stocks in the same sector.

The paper is organized as follows. In Section 2, we introduce the new factor correlation model, which features a novel variation-free parametrization of factor loadings and a (sparse) block idiosyncratic correlation matrix. In Section 3, we present details about the convolution- t distributions and the particular variants we use in the empirical analysis. In Section 4, we develop the score-driven dynamic models for two estimation methods (joint and decoupled), and provide analytical expressions for the score and information matrix across a range of convolution- t distributions and structures for the idiosyncratic correlation matrices. We present the empirical analysis in Section 5 and conclude in Section 6. All proofs are provided in the Appendix.

2 The Factor Correlation Model

Let $\{\mathcal{F}_t\}$ be a filtration and R_t is an n -dimensional return vector adapted to \mathcal{F}_t . We denote the conditional mean and the conditional covariance matrix by $\mu_t = \mathbb{E}(R_t|\mathcal{F}_{t-1})$ and $\Sigma_t = \text{var}(R_t|\mathcal{F}_{t-1})$, respectively. We use the diagonal elements of the latter, $\sigma_{it}^2 = \text{var}(R_{it}|\mathcal{F}_{t-1})$,

$i = 1, \dots, n$, to define the diagonal matrix of conditional volatilities, $\Lambda_{\sigma_t} \equiv \text{diag}(\sigma_{1t}, \dots, \sigma_{nt})$, such that the conditional correlation matrix of R_t is given by $C_t = \Lambda_{\sigma_t}^{-1} \Sigma_t \Lambda_{\sigma_t}^{-1}$.

We adopt the spirit of the Dynamic Conditional Correlation (DCC) model by Engle (2002) that models the conditional variances and conditional correlations separately. Each of the n univariate return series is modeled with a univariate GARCH model (we use EGARCH models in empirical analysis). From the resulting conditional moments, μ_{it} and σ_{it} , we define the vector of standardized returns, $Z_t = \Lambda_{\sigma_t}^{-1}(R_t - \mu_t) \sim (0, C_t)$. Similarly, we define the standardized factor variables, $F_{jt} = \sigma_{f_j,t}^{-1}(R_{f_j,t} - \mu_{f_j})$ for $j = 1, \dots, r$, such that $F_t \sim (0, C_{F,t})$.

We have little to add to the large existing literature on univariate GARCH models. We will therefore take the univariate GARCH models as given, and treat Z_t and F_t as the observed data. Our focus is on the modeling of the conditional correlation matrix, $C_t = \text{var}_{t-1}(Z_t)$ using the observed factor variables F_t .

A central component of our model is a factor structure,

$$Z_{it} = \beta'_{it} F_t + \omega_{it} e_{it}, \quad e_{it} \sim (0, 1) \quad (1)$$

for $i = 1, \dots, n$ and $t = 1, \dots, T$, where e_{it} is an idiosyncratic shock and ω_{it}^2 is the proportion of variance attributed to the idiosyncratic component. To simplify the notation, we suppress the dependence on t in most of Sections 2 and 3, such that (1) is expressed as $Z_i = \beta'_i F + \omega_i e_i$. We will reintroduce subscript- t again once the dynamic model is introduced.

From the standardized factor variables, $F \sim (0, C_F)$, we define the uncorrelated factor variables, $U = C_F^{-1/2} F \sim (0, I_r)$, where $C_F^{1/2}$ denotes the symmetric square-root of C_F .² This enables us to rewrite (1) as

$$Z_i = \rho'_i U + \omega_i e_i, \quad e_i \sim (0, 1) \quad (2)$$

where the elements of vector $\rho_i = C_F^{1/2} \beta_i$ are simply the correlation coefficients, as we have $\rho_i = [\text{corr}(Z_i, U_1), \dots, \text{corr}(Z_i, U_r)]'$. It now follows that $\omega_i = \sqrt{1 - \rho'_i \rho_i}$. In matrix form the model can be expressed as

$$Z = \boldsymbol{\rho}' U + \Lambda_\omega e, \quad e \sim (0, C_e) \quad (3)$$

where $\boldsymbol{\rho} = [\rho_1, \dots, \rho_n] \in \mathbb{R}^{r \times n}$, $\Lambda_\omega = \text{diag}(\omega_1, \dots, \omega_n) \in \mathbb{R}^{n \times n}$, and e is the vector of idiosyncratic shocks. We will not require e to be cross-sectionally uncorrelated. However, we will introduce parsimonious and sparse structures on C_e . It follows that the conditional

²An attractive feature of $U = C_F^{-1/2} F$ is that it maximizes the average correlation between U_j and F_j , $j = 1, \dots, r$, which helps interpret the results based on U . There are other ways to define uncorrelated factor variables from F , such as those based on Cholesky decompositions. All choices are equivalent in terms of the implied factor loadings on F , β_i , $i = 1, \dots, n$.

correlation matrix for returns is given by,

$$C = \boldsymbol{\rho}'\boldsymbol{\rho} + \Lambda_\omega C_e \Lambda_\omega,$$

which is a generalization of [Hansen et al. \(2014\)](#) who focus on a single factor ($r = 1$).

The number of factors, r , is typically small relative to the number of assets n , which makes it straightforward to formulate a dynamic model for the conditional correlation matrix of the observed factors F , C_F . We adopt the score-driven multivariate GARCH model by [Tong et al. \(2024\)](#) for this purpose.

The conditional model of Z given U is the central component of the proposed model, and we will refer to this as the *Core Correlation Model*. The key parameters in the core correlation model are the factor loading parameters, $\boldsymbol{\rho} \in \mathbb{R}^{r \times n}$, and the correlation matrix for the idiosyncratic shocks, C_e . (The scaling matrix, Λ_ω , is a function of $\boldsymbol{\rho}$). The main obstacle to a dynamic model of factor loadings is the requirement: $\rho'_i \rho_i < 1$ for $i = 1, 2, \dots, n$. We resolve this by introducing a novel and mathematically elegant reparametrization of ρ_i , $i = 1, \dots, n$, which is inspired by the generalized Fisher transformation of correlation matrices, see [Archakov and Hansen \(2021\)](#). An overview of the model structure is illustrated in [Figure 2](#), which has many additional details related to distributions and estimation method that will be explained later in this paper.

2.1 A Novel Parametrization of Factor Loadings

The correlation structure in the factor correlation model, [\(3\)](#), is fully characterized by ρ_1, \dots, ρ_n and C_e , because $\omega_i = \sqrt{1 - \rho'_i \rho_i}$. This parametrization must satisfy $\rho'_i \rho_i < 1$ for all i . An alternative, variation-free parametrization of vector ρ_i is the following.

Theorem 1. *Let the correlation structure of $Z \in \mathbb{R}^n$ be given by [\(2\)](#), where $\rho'_i \rho_i < 1$ for all $i = 1, \dots, n$. Then*

$$\tau_i = \frac{\operatorname{artanh}(\sqrt{\rho'_i \rho_i})}{\sqrt{\rho'_i \rho_i}} \times \rho_i \in \mathbb{R}^r, \quad i = 1, \dots, n, \quad (4)$$

is a variation-free parametrization of ρ_i with domain $\tau = (\tau'_1, \dots, \tau'_n)' \in \mathbb{R}^{rn}$.

The inverse mapping and its Jacobian matrix are given by

$$\rho_i = \frac{\tanh(\sqrt{\tau'_i \tau_i})}{\sqrt{\tau'_i \tau_i}} \times \tau_i \quad i = 1, \dots, n.$$

and $J(\tau_i) \equiv \frac{\partial \rho_i}{\partial \tau'_i} = \sqrt{\frac{\rho'_i \rho_i}{\tau'_i \tau_i}} P_{\tau_i}^\perp + (1 - \rho'_i \rho_i) P_{\tau_i}$, respectively, where $P_{\tau_i} = \tau_i (\tau'_i \tau_i)^{-1} \tau'_i$ and $P_{\tau_i}^\perp = I_r - P_{\tau_i}$ are orthogonal projection matrices.

The unrestricted τ -parametrization in Theorem 1 is inspired by the new parametrization of correlation matrices in Archakov and Hansen (2021). We apply the matrix logarithm to

$$C_i^* = \text{corr} \begin{pmatrix} Z_i \\ U \end{pmatrix} = \begin{bmatrix} 1 & \rho'_i \\ \rho_i & I_r \end{bmatrix}, \quad (5)$$

which is given by

$$\log C_i^* = \frac{1}{2} \begin{bmatrix} \log(1 - \rho'_i \rho_i) & \frac{1}{\sqrt{\rho'_i \rho_i}} \log \left(\frac{1 + \sqrt{\rho'_i \rho_i}}{1 - \sqrt{\rho'_i \rho_i}} \right) \rho'_i \\ \frac{1}{\sqrt{\rho'_i \rho_i}} \log \left(\frac{1 + \sqrt{\rho'_i \rho_i}}{1 - \sqrt{\rho'_i \rho_i}} \right) \rho_i & \frac{1}{\rho'_i \rho_i} \log(1 - \rho'_i \rho_i) (\rho_i \rho'_i) \end{bmatrix},$$

as shown in Appendix A. Here we use the convention $\log C^* = 0$ if $\rho_i = 0 \in \mathbb{R}^r$. An interesting observation is that $\text{arctanh}(\sqrt{\rho'_i \rho_i}) = \frac{1}{2} \log \left(\frac{1 + \sqrt{\rho'_i \rho_i}}{1 - \sqrt{\rho'_i \rho_i}} \right)$ is the Fisher transformation of $\sqrt{\rho'_i \rho_i}$ (the root of sum of squares factor loadings).

The τ -parametrization in Theorem 1 is useful for several reasons. First, it makes it easy to impose sparsity and other structure on C_i^* because ρ_i is proportional to τ_i , such that $\rho_{i,j} = 0 \Leftrightarrow \tau_{i,j} = 0$ and $\rho_{i,j} = \rho_{i,j'} \Leftrightarrow \tau_{i,j} = \tau_{i,j'}$. Moreover, we also have $\rho_i = \rho_{i'} \Leftrightarrow \tau_i = \tau_{i'}$ which shows that two assets have identical factor loadings if and only if the corresponding τ -vectors are identical. This makes it easy to impose group structures on the factor loadings. That the Jacobian, J , is symmetric and easy to compute will also be convenient in the dynamic score-driven model of ρ_i .

Remark (Notation of Factor Parametrizations). We use $\boldsymbol{\rho} = (\rho_1, \dots, \rho_n)$ to denote the $r \times n$ matrix of factor loadings and let $\rho = \text{vec}(\boldsymbol{\rho}) = (\rho'_1, \dots, \rho'_n)' \in \mathbb{R}^{rn}$ be the vector with stacked factor loadings. Similarly, we use $\tau = (\tau'_1, \dots, \tau'_n)' \in \mathbb{R}^{rn}$.

2.2 Idiosyncratic Correlation Matrix

The $n \times n$ correlation matrix for the idiosyncratic component, $C_e = \text{corr}(e)$, has $d = n(n-1)/2$ correlations. A dynamic model for C_e will therefore need some structure to be imposed, unless n is small. In this context, a simple and convenient structure is to impose block structures on C_e , that can be easily combined with sparsity assumptions. Dynamic block correlation matrices were introduced by Engle and Kelly (2012), and the canonical representation of block matrices by Archakov and Hansen (2024) made it possible to apply this structure to matrices with more than 2×2 blocks, and greatly simplified estimation and guaranteeing positive definiteness.

Below we adopt notations from Tong et al. (2024), but should emphasize that our model

structure is very different from that in [Tong et al. \(2024\)](#), because they do not incorporate observable factors. They impose the block structures directly on $C = \text{corr}(Z)$, whereas we impose the block structure on in idiosyncratic correlation matrix, $C_e = \text{corr}(e)$.

2.2.1 Block Correlation Matrices

A block correlation matrix is defined by partitioning the variables into K groups, where the correlation between any two variables depends solely on their group assignments. Let n_k denote the number of variables in the k -th group for $k = 1, \dots, K$, such that $n = \sum_{k=1}^K n_k$. Define $\mathbf{n} = (n_1, n_2, \dots, n_K)'$ as the vector of group sizes. We assume that the variables are sorted such that the first n_1 variables belong to the first group, the next n_2 variables belong to the second group, and so on.

The block structure on C_e can be expressed with

$$C_e = \begin{bmatrix} C_{[1,1]} & C_{[1,2]} & \cdots & C_{[1,K]} \\ C_{[2,1]} & C_{[2,2]} & & \\ \vdots & & \ddots & \\ C_{[K,1]} & & & C_{[K,K]} \end{bmatrix},$$

where $C_{[k,l]}$ is an $n_k \times n_l$ matrix given by

$$C_{[k,l]} = \begin{bmatrix} \rho_{kl} & \cdots & \rho_{kl} \\ \vdots & \ddots & \vdots \\ \rho_{kl} & \cdots & \rho_{kl} \end{bmatrix}, \text{ for } k \neq l \quad \text{and } C_{[k,k]} = \begin{bmatrix} 1 & \rho_{kk} & \cdots & \rho_{kk} \\ \rho_{kk} & 1 & \ddots & \\ \vdots & \ddots & \ddots & \\ \rho_{kk} & & & 1 \end{bmatrix}.$$

Here we have omitted the subscript- e on the submatrices to simplify the expositions. Within each block, there is (at most) a single correlation coefficient, such that the block structure reduces the number of unique correlations from $d = n(n-1)/2$ to at most $K(K+1)/2$.³ This number does not increase with n , if K is held constant, and this makes it possible to scale the model to high dimensions.

We refer to this as the the block correlations structure or the Full Block Correlation (FBC) structure. In our empirical analysis we partition assets by subindustries (8 digit GICS codes) which is used to define the blocks in C_e . Sectors (2 digit GICS codes) will later be used to impose sparsity on C_e .

³This is based on the general case that the number of assets in each group is at least two. When there are $\tilde{K} \leq K$ clusters with only one asset, this number become $K(K+1)/2 - \tilde{K}$.

2.2.2 Sparse Block Correlation Matrices

We consider two particular types of sparse block correlation matrices that are based on a multi-level partitioning of the variables.

A Sparse Block Correlation (SBC) is based on a second, coarser partitioning that induces sparsity on the correlation matrix. We use GICS sectors to define the coarser partitioning in our empirical analysis. The Diagonal Block Correlation (DBC) structure imposes additional sparsity by imposing $C_{[k,l]} = 0$ for $k \neq l$. In our empirical analysis, this implies that idiosyncratic shocks for stocks in different subindustries are uncorrelated.

Examples of the four types of correlation structures are shown in Figure 1.

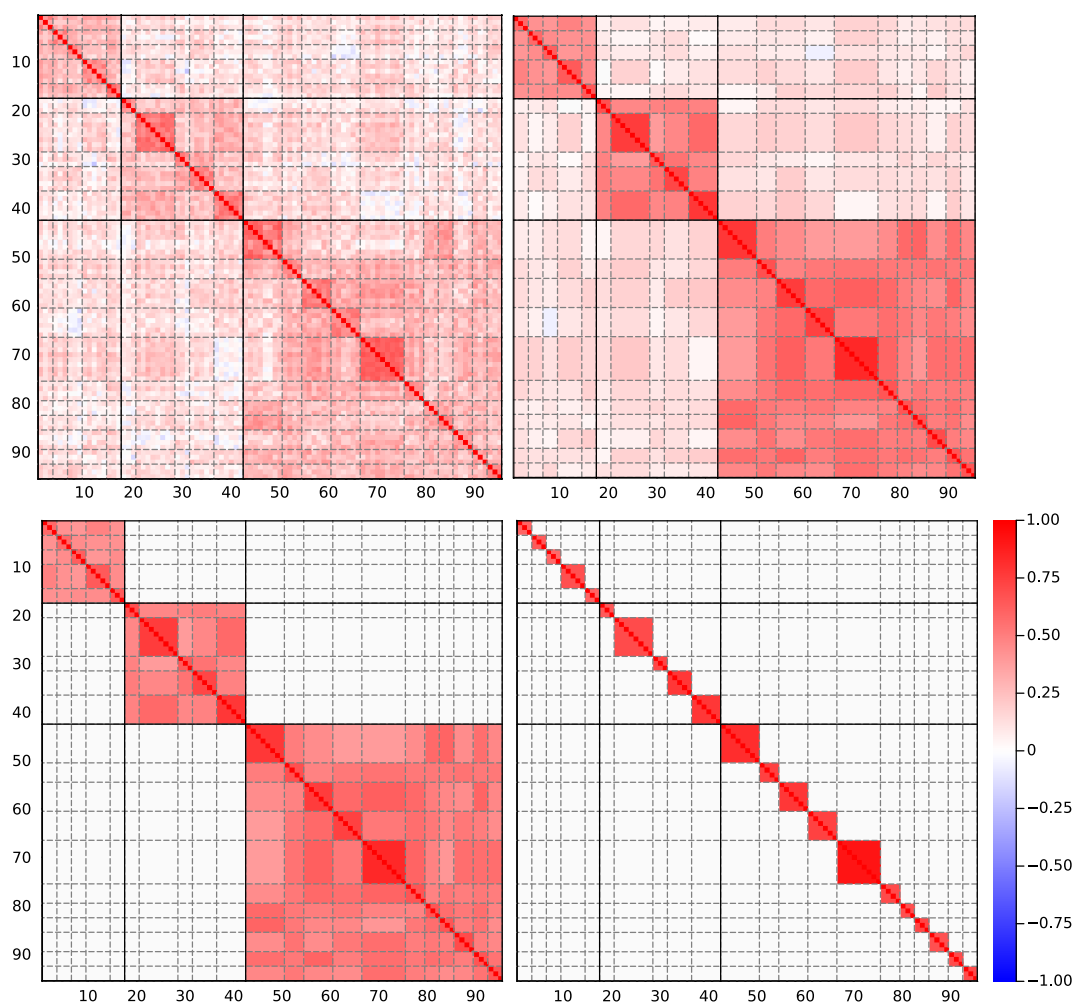


Figure 1: Examples of block correlation matrices. Upper-left: Unrestricted Correlation matrix. Upper-right: Block Correlation matrix with blocks defined by subindustries. Lower-left: Sparse Block Correlation matrix with zero correlations between sectors. Lower-right: Diagonal Block Correlation matrix.

2.3 Parametrizing the Idiosyncratic Correlation Matrix

We parameterize the idiosyncratic correlation matrix, C_e , using the generalized Fisher transformation by [Archakov and Hansen \(2021\)](#),

$$\gamma(C_e) \equiv \text{vecl}(\log C_e) \in \mathbb{R}^{n(n-1)/2}$$

where $\log C_e$ is the matrix logarithm of C_e and $\text{vecl}(\cdot)$ vectorizes the elements in the lower triangle of C_e (the elements below the diagonal).⁴ The following example illustrates this parametrization for an 3×3 correlation matrix:

$$\gamma \equiv \text{vecl} \left[\log \begin{pmatrix} 1.0 & \bullet & \bullet \\ 0.7 & 1.0 & \bullet \\ 0.4 & 0.6 & 1.0 \end{pmatrix} \right] = \text{vecl} \left[\begin{pmatrix} -.35 & \bullet & \bullet \\ .825 & -.53 & \bullet \\ .223 & .642 & -.24 \end{pmatrix} \right] = \begin{pmatrix} .825 \\ .223 \\ .642 \end{pmatrix}.$$

This parametrization defines a one-to-one mapping between $\mathbb{R}^{n(n-1)/2}$ and the set of positive definite correlation matrices, see [Archakov and Hansen \(2021\)](#). The matrix logarithm preserves block structures, as illustrated with,

$$\underbrace{\begin{bmatrix} 1.0 & 0.8 & 0.4 & 0.4 \\ 0.8 & 1.0 & 0.4 & 0.4 \\ 0.4 & 0.4 & 1.0 & 0.6 \\ 0.4 & 0.4 & 0.6 & 1.0 \end{bmatrix}}_{=C_e} \implies \underbrace{\begin{bmatrix} -.57 & 1.02 & .256 & .256 \\ 1.02 & -.57 & .256 & .256 \\ .256 & .256 & -.29 & .628 \\ .256 & .256 & .628 & -.29 \end{bmatrix}}_{=\log C_e}.$$

For a block matrix with K blocks, $\gamma(C_e)$ will have at most $(K + 1)K/2$ distinct elements, such that we can write $\gamma = B\eta$, where B is a known bit-matrix and η is a subvector of γ . In the example above we have,

$$\gamma = B\eta, \quad B = \begin{pmatrix} 1 & 0 & 0 & 0 & 0 & 0 \\ 0 & 1 & 1 & 1 & 1 & 0 \\ 0 & 0 & 0 & 0 & 0 & 1 \end{pmatrix}, \quad \eta = \begin{pmatrix} 1.02 \\ .256 \\ .628 \end{pmatrix}.$$

Parametrizing the block correlation matrix, C_e , with η does not impose additional superfluous restrictions, see [Tong and Hansen \(2023\)](#). Thus, any non-singular block correlation matrix corresponds to a unique η vector, and any dynamic block correlation model can be expressed as a dynamic model for η .

For the two sparse correlation structures, SBC and DBC, $\log C_e$ will have the same

⁴One can define the matrix logarithm of a nonsingular correlation matrix, by $\log C_e = Q \log \Lambda Q'$, where $C_e = Q\Lambda Q'$ is the eigendecomposition of C_e .

sparse structure, with zeroes outside the diagonal blocks. The dimension of η can therefore be reduced substantially. For the DBC structure with K diagonal blocks, we can use $\eta = (\eta_1, \dots, \eta_K)'$, where

$$\eta_k = \frac{1}{n_k} \log \left(1 + n_k \frac{\varrho_{kk}}{1 - \varrho_{kk}} \right), \quad k = 1, \dots, K, \quad (6)$$

see [Archakov and Hansen \(2021, proposition 2\)](#). This follows from $\eta_k = \log C_{[k,k]}$, where each diagonal block, $C_{[k,k]}$, is an equicorrelation matrix. For later use we observe that inverse transformation and its Jacobian are given by

$$\varrho_{kk} = \frac{\exp(n_k \eta_k) - 1}{\exp(n_k \eta_k) + n_k - 1}, \quad \text{and} \quad J_k = \frac{\partial \varrho_{kk}}{\partial \eta_k} = \frac{1}{(1 - \varrho_{kk})(1 + (n_k - 1)\varrho_{kk})}.$$

So, the analysis is greatly simplified with the DBC structure for C_e , even in very high-dimensional settings.

For SBC correlation structure, we can apply the results for block correlation matrices to each of the big diagonal blocks separately, and combining the η s for each block to define η .

2.3.1 Canonical Form of Idiosyncratic Correlation Matrix

To build a score-driven model for block correlation matrix, the conventional way is to use

$$\frac{\partial \ell}{\partial \eta'} = \frac{\partial \ell}{\partial \gamma'} \frac{\partial \gamma}{\partial \eta'} = \frac{\partial \ell}{\partial \gamma'} B \quad (7)$$

where $\gamma = \text{vecl}(\log C_e) \in \mathbb{R}^{n(n-1)/2}$ and ℓ is the log-likelihood function. Therefore, even if C_e has a block structure with unique value η with at most $K(K+1)/2$ elements, the conventional way through (7) also involves the computation of $n \times n$ matrix, which doesn't take the advantages of block structure of C_e . In fact, expect for diagonal block correlation matrix which can be modeled through unrestricted η_k for each $k = 1, 2, \dots, K$, the modeling of a general block correlation matrix C_e including the SBC case, both requires the following canonical representation of block correlation matrix, such that the related computation only involves the K -dimensional matrix. The canonical representation of block correlation matrix resembles the eigendecomposition of matrices, see [Archakov and Hansen \(2024\)](#). For a block correlation matrix with block-sizes, (n_1, \dots, n_K) , we have

$$C_e = QDQ', \quad D = \begin{bmatrix} A & 0 & \cdots & 0 \\ 0 & \delta_1 I_{n_1-1} & \ddots & \vdots \\ \vdots & \ddots & \ddots & 0 \\ 0 & \cdots & 0 & \delta_K I_{n_K-1} \end{bmatrix}, \quad \delta_k = \frac{n_k - A_{kk}}{n_k - 1} \quad (8)$$

where $A \in \mathbb{R}^{K \times K}$ with $A_{kk} = 1 + (n_k - 1) \rho_{kk}$, and $A_{kl} = \rho_{kl} \sqrt{n_k n_l}$ for $k \neq l$. Matrix Q is a cluster-specific orthonormal matrix, $Q'Q = QQ' = I_n$, which is solely determined by the block sizes, (n_1, \dots, n_K) , such that it does not depend on C_e . Computing the powers of C_e , including the matrix inverse, logarithm and the exponential, is greatly simplified as they only involve the calculations related to $K \times K$ matrix A . From [Archakov and Hansen \(2024, corollary 2\)](#), the unique values in $\gamma(C_e)$, i.e. the elements in η , can be expressed as

$$\eta = L_K(\Lambda_n^{-1} \otimes \Lambda_n^{-1})\text{vec}(W), \quad (9)$$

where $W = \log A - \log \Lambda_\delta$, where $\Lambda_\delta = \text{diag}(\delta_1, \dots, \delta_K)$ and $\Lambda_n = \text{diag}(\sqrt{n_1}, \dots, \sqrt{n_K})$ are diagonal matrices. L_K is the elimination matrix, that solves $\text{vech}(A) = L_K \text{vec}(A)$, and \otimes is the Kronecker product. The canonical representation greatly facilitates the evaluation of likelihood function and the computation of score. [Tong et al. \(2024\)](#) build a score driven model for a general block correlation matrix by utilizing the canonical form (8) and (9).

3 Distributions

The class of distributions we consider in our empirical analysis is detailed in this section. We adopt the family of convolution- t distributions of [Hansen and Tong \(2024\)](#). These can accommodate nonlinear dependencies and heterogeneous marginal distributions. This class of distributions nests the multivariate t -distributions (including Gaussian distributions) as special cases. A convolution- t distribution has a relatively simple log-likelihood function, and we adopt this distribution for both the factor variables, $F \sim (0, C_F)$, and the idiosyncratic shocks, $e \sim (0, C_e)$. Under the assumption that e and F are independent, the conditional distribution of Z given F is also a convolution- t distribution.

3.1 The Convolution- t Distribution

Let X be a random vector with mean, $\mu = \mathbb{E}[X]$, and covariance matrix, $\Sigma = \text{var}(X)$. We use X to represent either F , $Z|U$ or e , and write

$$X = \mu + \Xi V \sim \text{CT}_{m, \nu}^{\text{std}}(\mu, \Xi), \quad \text{where } \Xi \Xi' = \Sigma,$$

which follows the notation in [Hansen and Tong \(2024\)](#). A convolution- t distribution is (aside from location and scale) a rotation of a random vector, $V = (V_1', \dots, V_G')' \in \mathbb{R}^n$, which consists of G mutually independent multivariate t -distributions, where $V_g \sim t_{\nu_g}^{\text{std}}(0, I_{m_g})$ has dimension m_g and degrees of freedom, $\nu_g > 2$, for $g = 1, \dots, G$ and with $n = \sum_{g=1}^G m_g$. Here

$\boldsymbol{\nu} = (\nu_1, \dots, \nu_G)'$ is the vector with degrees of freedom and $\mathbf{m} = (m_1, \dots, m_G)'$ is the vector with the dimensions for the G multivariate t -distributions. The corresponding log-likelihood function is surprisingly simple. Set $V = \Xi^{-1}(X - \mu)$, then

$$\ell(X) = -\log |\Xi| + \sum_{g=1}^G c_g - \frac{\nu_g + m_g}{2} \log \left(1 + \frac{1}{\nu_g - 2} V_g' V_g \right), \quad (10)$$

where $c_g = c(\nu_g, m_g) = \log \left(\Gamma \left(\frac{\nu_g + m_g}{2} \right) / \Gamma \left(\frac{\nu_g}{2} \right) \right) - \frac{m_g}{2} \log [(\nu_g - 2)\pi]$, $g = 1, \dots, G$, are the normalizing constants in the multivariate t -distribution. Note that we previously used a partitioning of the variables, $n = (n_1, \dots, n_K)'$, to form a block correlation structure. The convolution- t distribution involves a second partitioning that defines the G independent multivariate t -distributions. This is a cluster structure for nonlinear dependences in the underlying random innovations. The two cluster structures can be different or identical.

Next, we highlight five distributional properties of this model. First, each element of $V_g \in \mathbb{R}^{m_g}$ follows the same marginal t -distribution with ν_g degrees of freedom. This is not necessarily true for the elements of X , as they are typically unique convolutions of the G underlying t -distributions. Second, the marginal distributions of X may be time-varying, as they depend on Ξ , which can change over time in the model. Third, the elements of X have intricate dependencies, arising from the common t -distributions they share. These dependencies induce tail correlations and can include cluster-specific tail dependencies. Fourth, increasing the number of G -clusters does not always improve the empirical fit. While a larger G increases the number of degrees-of-freedom parameters, it also divides V into a larger number of independent subvectors, which removes the intrinsic dependence between elements of V that were previously part of the same multivariate t -distribution. Fifth, this model nests the conventional multivariate t -distribution as a special case when $G = 1$, facilitating straightforward comparisons with a natural benchmark model, such as the multivariate Gaussian distribution.

3.2 Three Special Convolution- t Distributions

The convolution- t distributions define a broad class of distributions, as V can be partitioned in many ways. We will use three particular types of convolution- t distributions, one being the standard multivariate t -distribution.

3.2.1 Multivariate- t Distribution (MT)

The convolution- t distributions nests the multivariate t -distribution as a special case. The n -dimensional (standardized) multivariate t -distribution is denoted, $X \sim t_v^{\text{std}}(\mu, \Sigma)$, where

$\nu > 2$ is the degrees of freedom. The corresponding log-likelihood is given by

$$\ell(X) = c_{\nu,n} - \frac{1}{2} \log |\Sigma| - \frac{\nu+n}{2} \log \left(1 + \frac{1}{\nu-2} (X - \mu)' \Sigma^{-1} (X - \mu) \right), \quad \nu > 2. \quad (11)$$

As $\nu \rightarrow \infty$, the multivariate t -distribution approaches the multivariate normal distribution, $N(\mu, \Sigma)$. The main advantage of using the standardized t -distribution is that $\text{var}(X) = \Sigma$. If X is standardized and $\Sigma = C$ has a block structure with K clusters, we can use the canonical representation in Section 2.3.1 of to obtain the following simplified expression,

$$\ell(X) = c_{\nu,n} - \frac{1}{2} \log |A| - \frac{1}{2} \sum_{k=1}^K (n_k - 1) \log \delta_k - \frac{\nu+n}{2} \log \left[1 + \frac{1}{\nu-2} \left(Y_0' A^{-1} Y_0 + \sum_{k=1}^K \frac{1}{\delta_k} Y_k' Y_k \right) \right].$$

where $Y = Q'(X - \mu)$. The multivariate t -distribution has two potential drawbacks. First, all elements of a multivariate t -distribution are dependent, because they share a common random mixing variable. Second, all elements of V are identically distributed, because they are all t -distributed with the same degrees of freedom. Both implications may be too restrictive in many applications, especially if the dimension, n , is large.

3.2.2 Cluster- t Distribution (CT)

The second special type of convolution- t distribution is called the Cluster- t (CT) distribution. It has a cluster structure on V , represented by \mathbf{m} . In the absence of a block structure on Ξ , the log-likelihood function is computed by (10). If X is standardized, $\Sigma = C$ has a block structure with $\mathbf{n} = \mathbf{m}$ and $G = K$, and we set $\Xi = C^{1/2}$, then we have,

$$V_k' V_k = Y_0' A^{-\frac{1}{2}} e_k e_k' A^{-\frac{1}{2}} Y_0 + \delta_k^{-1} Y_k' Y_k, \quad k = 1, \dots, K,$$

where $Y = Q'(X - \mu) = (Y_0', Y_1', \dots, Y_K')'$ and the log-likelihood function simplifies to

$$\ell(X) = -\frac{1}{2} \log |A| + \sum_{k=1}^K c_k - \frac{1}{2} (n_k - 1) \log \delta_k - \frac{\nu_k + n_k}{2} \log \left(1 + \frac{1}{\nu_k - 2} V_k' V_k \right),$$

where $c_k = c(\nu_k, n_k)$. The block structure simplifies implementation of the score-driven model for this specification, and makes it possible to apply in high dimensions.

3.2.3 Convolution of Heterogeneous t -distributions (HT)

The third special type of convolution- t distributions has $G = n$. So, the elements of V are made up of n independent univariate t -distributions with degrees of freedom, ν_i , $i = 1, \dots, n$. This distribution can accommodate a high degree of heterogeneity in the marginal

properties of X_i , $i = 1, \dots, n$, which are different convolutions of heterogeneous independent t -distributions. For this reason, we refer to these as HT distributions, where H is short for heterogeneous. The number of degrees of freedom increases from G to n , but the additional parameters do not guarantee a better in-sample log-likelihood, because dependences between elements of V is eliminated. Without structure on Σ , the log-likelihood function is simply computed by (10). As before, if X is standardized, $\Sigma = C$ has a block structure with group assignments \mathbf{n} , and we set $\Xi = C^{1/2}$, then the log-likelihood function simplifies to

$$\ell(X) = c - \frac{1}{2} \log |A| - \frac{1}{2} \sum_{k=1}^K (n_k - 1) \log \lambda_k - \sum_{k=1}^K \sum_{j=1}^{n_k} \frac{\nu_{k,j} + 1}{2} \log \left(1 + \frac{1}{\nu_{k,j} - 2} V_{k,j}^2 \right),$$

where $c = \sum_{i=1}^n c(\nu_i, 1)$ and $V_{k,j}$ is the j -th element of the vector V_k .

4 Model Architecture and Components

Individual returns and factor returns are model with univariate GARCH models that define the standardized variables, Z_t and F_t . The dynamic model of (Z_t, F_t) has several components. The first is the dynamic model of $C_F = \text{corr}(F_t)$, which is a score-driven model of $\gamma(C_f)$, and this model delivers the orthogonalized factor variables, U_t . The most innovative component is the way we model dynamic factor loadings with the τ -parametrization. This is part of the core correlation model, which also include the dynamic model of the idiosyncratic correlation matrix, C_e . The two components of the core correlation model can be estimated jointly or separately, where we refer to the latter as decoupled estimation. An overview of the structure of the factor correlation model is illustrated in Figure 2.

4.1 Univariate Volatility Models for Returns Series

The factor correlation model requires standardized returns, $Z_{i,t}$, $i = 1, \dots, n$ and standardized factor variables, $F_{j,t}$, $j = 1, \dots, r$. Each of these are obtained from suitable univariate models for the conditional mean and variance of their corresponding return series.

There is a wide range of choices for the univariate volatility models that serve this purpose, see e.g. Hansen and Lunde (2005). We do not contribute to this modeling aspect. In our empirical analysis we simply use univariate EGARCH model, see Nelson (1991), to standardized each returns series, from which we obtain $Z_t \in \mathbb{R}^n$ and $F_t \in \mathbb{R}^r$.

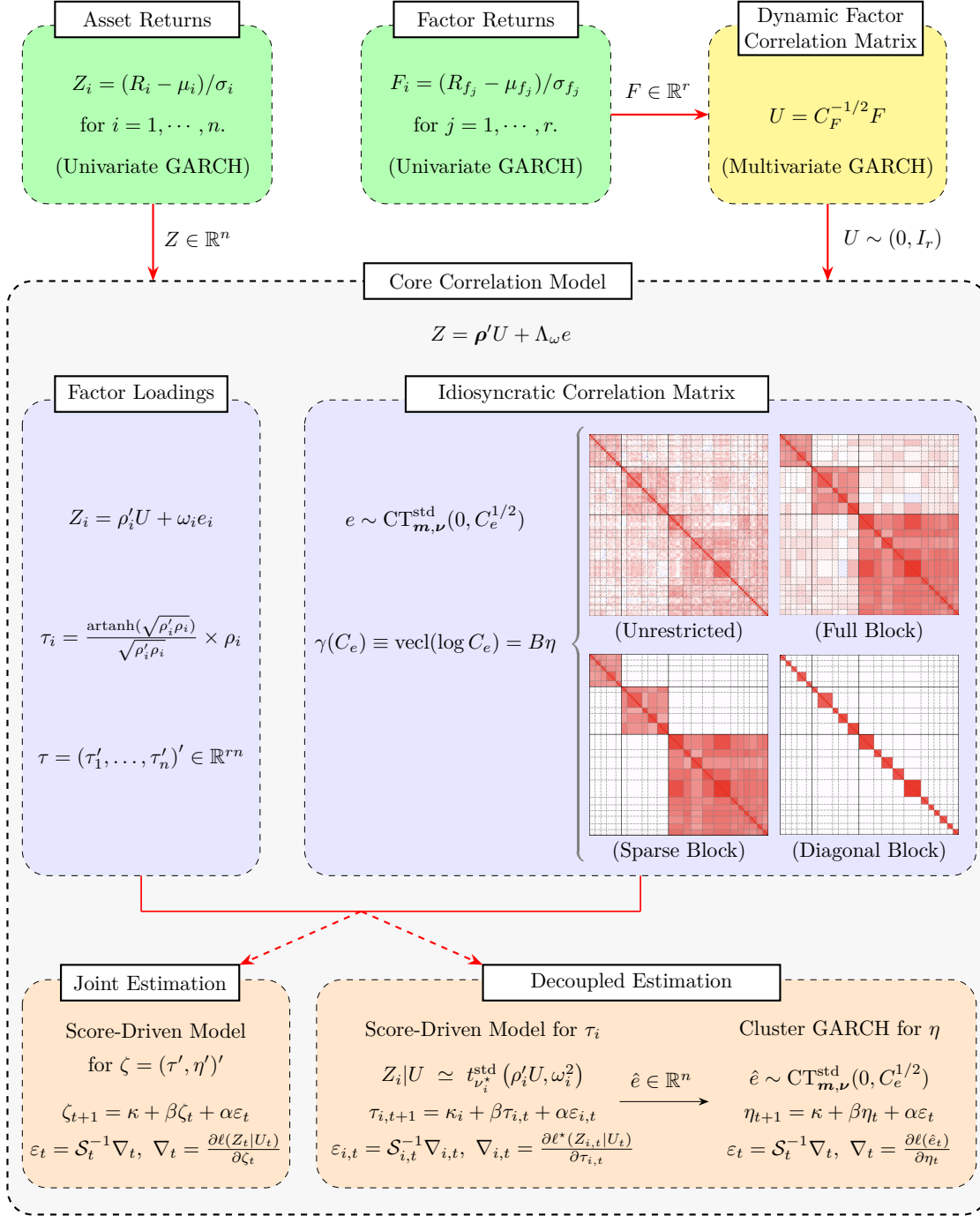


Figure 2: Model architecture and components. The primary methodological contribution in this paper is the core correlation model.

4.2 Model for Standardized Factor Variables

We model the standardized factor variables, F_t , using the score-driven model by [Tong et al. \(2024\)](#). Because r is relatively small, there is not need to impose structure on $C_{F_t} = \text{corr}(F_t)$. The score-drive framework was introduced by [Creal et al. \(2013\)](#), where dynamic parameters are updated based on the score of the log-likelihood function. Here we specify a score-model for the vector representation of the correlation matrix, $\gamma_t^F = \text{vecl}(\log C_{F_t})$, specifically

$$\gamma_{t+1}^F = \kappa^F + \beta^F \gamma_t^F + \alpha^F \varepsilon_t^F,$$

where $\kappa^F = (I_{r(r-1)/2} - \beta^F)\mu^F$ with $\mu^F = \mathbb{E}[\gamma_t^F]$, and α^F and β^F are $r(r-1)/2 \times r(r-1)/2$ matrices and $\varepsilon_t^F = \mathcal{S}_t^{-1} \nabla_{\gamma_t^F}$ where \mathcal{S}_t is a scaling matrix and, $\nabla_{\gamma_t^F} = \partial \ell(F_t) / \partial \gamma_t^F$, is the score of the log-likelihood function. The distributional assumption is that $F_t = C_{F_t}^{1/2} U_t$ with $U_t \sim \text{CT}_{d,\nu^F}^{\text{std}}(0, I_d)$, and we consider three types of distributions for U_t : Gaussian, Multivariate- t (MT), and (HT) distributions.

4.3 Dynamic Factor Loadings and Idiosyncratic Correlations

The *core correlation model* includes the dynamic models of factor loadings and the idiosyncratic correlation matrix. This is the central part of the proposed model, which describes the conditional distribution of Z_t given U_t , which involves dynamic factor loadings and a dynamic idiosyncratic correlation matrix with various structures. We adopt the convolution- t distribution with $\Xi = C_e^{1/2}$ for this part of the model, such that

$$Z = \boldsymbol{\rho}' U + \Lambda_\omega e, \quad e \sim \text{CT}_{m,\nu}^{\text{std}}(0, C_e^{1/2}), \quad (12)$$

Here $C_e^{1/2}$ is the symmetric square-root of C_e , and it follows that $Z|U \sim \text{CT}_{m,\nu}^{\text{std}}(\boldsymbol{\rho}' U, \Lambda_\omega C_e^{1/2})$. We parametrize the factor loadings by τ , whereas the idiosyncratic correlation matrix is parametrized by η , using various types of block structures, $\gamma(C_e) = B\eta$. Since Λ_ω is a function of $\boldsymbol{\rho}$, the parameters dynamic parameters are represented by the vector, $\zeta_t = (\tau_t', \eta_t')'$, which leads to a second score-driven model,

$$\zeta_{t+1} = \kappa + \beta \zeta_t + \alpha \varepsilon_t, \quad (13)$$

where β and α are coefficient matrices, $\kappa = (I_p - \beta)\mu_\zeta$ with $\mu_\zeta = \mathbb{E}[\zeta_t]$, and ε_t is defined by the score in period t .⁵ In the empirical analysis we let β and α be diagonal matrices to keep

⁵It is straightforward to include additional lagged values of ζ_t , such that (13) has a higher-order VAR(p) structure, and adding q lagged values of ε_t , would generalize (13) to a VARMA(p,q) model, we do not pursue

the model relatively parsimonious.

A key aspect of a score-driven model is the innovation, $\varepsilon_t = \mathcal{S}_t^{-1} \nabla_{\zeta_t}$, where $\nabla_{\zeta_t} = \partial \ell(Z_t|U_t)/\partial \zeta_t$ is the score of the predictive log-likelihood function and \mathcal{S}^{-1} is a suitable scaling matrix. This model structure is very intuitive, because (13) continuously updates ζ_t in the direction dictated by the first-order conditions of the log-likelihood.

To simplify the expositions, we suppress subscript- t in the rest of this Section. For the convolution- t distribution we need the following result that follows from Tong et al. (2024, theorems 5 and 6).

Lemma 1. *Suppose that $X \sim \text{CT}_{\mathbf{m}, \nu}^{\text{std}}(\mu, \Xi)$ and define $V = (V_1, \dots, V_G) = \Xi^{-1}(X - \mu)$, where $V_g \in \mathbb{R}^{n \times m_g}$ with $\sum_{g=1}^G m_g = n$. The partial derivatives (scores) with respect to μ and $\text{vec}(\Xi)$ are given by*

$$\nabla_{\mu} = \sum_{g=1}^G W_g \Xi'^{-1} P_g V_g, \quad \nabla_{\Xi} = \sum_{g=1}^G W_g \text{vec}(\Xi'^{-1} P_g V_g V_g') - \text{vec}(\Xi'^{-1}),$$

respectively, where $W_g = \frac{\nu_g + m_g}{\nu_g - 2 + V_g' V_g}$. The corresponding terms in the information matrix are

$$\begin{aligned} \mathcal{I}_{\mu} &= \sum_{g=1}^G \frac{(\nu_g + m_g) \nu_g}{(\nu_g + m_g + 2)(\nu_g - 2)} \Xi'^{-1} P_g P_g' \Xi^{-1}, \\ \mathcal{I}_{\Xi} &= (I_n \otimes \Xi'^{-1}) (K_n + \Upsilon_G) (I_n \otimes \Xi^{-1}), \end{aligned}$$

and $\mathcal{I}_{\mu \Xi} = 0$, where K_n is the commutation matrix, P_g is a $n \times m_g$ matrix from identity matrix $I_n = (P_1, \dots, P_G)$, and Υ_G is related to \mathbf{m} and ν , see Tong et al. (2024).

Note that W_g mitigates the influence that an outlier in V_g has on the scores. For latter use, we define

$$\xi \equiv \begin{pmatrix} \text{vec}(\mu, \omega)' \\ \eta \end{pmatrix}, \quad \text{and} \quad \Pi \equiv \frac{\partial \xi}{\partial \zeta'} = \begin{pmatrix} M & \mathbf{0} \\ \mathbf{0} & I \end{pmatrix}, \quad \text{where } M = \frac{\partial \text{vec}(\mu, \omega)'}{\partial \tau'}, \quad (14)$$

where $\mu = \boldsymbol{\rho}' U$ and $\omega = (\omega_1, \omega_2, \dots, \omega_n)'$ with $\omega_i = \sqrt{1 - \rho_i' \rho_i}$ for $i = 1, \dots, n$. Next, the following Theorem provides expressions for key terms in the score-driven model.

Theorem 2 (Key terms in Score-Driven Correlation Model). *Suppose that $e \sim \text{CT}_{\mathbf{m}, \nu}^{\text{std}}(0, C_e^{1/2})$ such that $Z|U \sim \text{CT}_{\mathbf{m}, \nu}^{\text{std}}(\mu, \Xi)$ with $\mu = \boldsymbol{\rho}' U$ and $\Xi = \Lambda_{\omega} C_e^{1/2}$, then the score vector and in-*

these extensions in this paper.

formation matrix with respect to the dynamic parameter, ζ , are given by

$$\nabla_{\zeta} = \Pi' \nabla_{\xi}, \quad \mathcal{I}_{\zeta} = \Pi' \mathcal{I}_{\xi} \Pi,$$

where

$$\nabla_{\xi} = \Theta' \begin{pmatrix} \nabla_{\mu} \\ \nabla_{\Xi} \end{pmatrix}, \quad \mathcal{I}_{\xi} = \Theta' \begin{pmatrix} \mathcal{I}_{\mu} & 0 \\ 0 & \mathcal{I}_{\Xi} \end{pmatrix} \Theta.$$

with $\theta = [\mu', \text{vec}(\Xi)']'$, we have

$$\Theta = \frac{\partial \theta}{\partial \xi'} = \begin{bmatrix} I_n & \mathbf{0} & \mathbf{0} \\ \mathbf{0} & \frac{\partial \text{vec}(\Xi)}{\partial \omega'} & \frac{\partial \text{vec}(\Xi)}{\partial \eta'} \end{bmatrix} \begin{bmatrix} K_{2n} & \mathbf{0} \\ \mathbf{0} & I_{n(n-1)/2} \end{bmatrix},$$

where K_{2n} is the communication matrix and

$$\frac{\partial \text{vec}(\Xi)}{\partial \omega'} = (C_e^{1/2} \otimes I_n) E_d', \quad \frac{\partial \text{vec}(\Xi)}{\partial \eta'} = (I_n \otimes \Lambda_{\omega})(C_e^{1/2} \oplus I_n)^{-1} \frac{\partial \text{vec}(C_e)}{\partial \gamma'} B.$$

where E_d is the elimination matrix such that $\text{diag}(S) = E_d \text{vec}(S)$ for any square matrix S .

The expression for $\partial \text{vec}(C_e) / \partial \gamma'$ is in Appendix A. The matrix M in (14) is given by

$$M = K_{n2} \begin{bmatrix} (U' \otimes I_n) \sum_{i=1}^n (I_d \otimes P_i) J_i (P_i' \otimes I_d) \\ -\frac{1}{2} \Lambda_{\omega}^{-1} E_d (I_{n^2} + K_n) (\boldsymbol{\rho}' \otimes I_n) \sum_{i=1}^n (I_d \otimes P_i) J_i (P_i' \otimes I_d) \end{bmatrix},$$

where P_i is the i -th column of identity matrix I_n , and J_i is the Jacobian matrix $\partial \rho_i / \partial \tau_i$.

Proof. See Appendix A. □

A common choice for the scaling matrix is the Fisher information $S_t = \mathcal{I}_{\zeta_t} = \mathbb{E}(\nabla_{\zeta_t} \nabla'_{\zeta_t})$, see Creal et al. (2013). However, in the present context, \mathcal{I}_{ζ_t} will not be invertible if $r \geq 2$, which stems from the conditional mean, $\rho_i' U$, being univariate, while ρ_i is r -dimensional.

A natural starting point is to use the Moore-Penrose inverse, \mathcal{I}_{ζ}^+ , of \mathcal{I}_{ζ} . Unfortunately, this choice turns out to be numerically unstable, as we explain in the next subsection.

4.3.1 Moore-Penrose Inverse of Information Matrix

Note that the parameter vector ξ defined in (14) is a minimal parameterization for the convolution- t distribution, and the information matrix for ζ can be expressed as $\mathcal{I}_{\zeta} = \Pi' \mathcal{I}_{\xi} \Pi$ with its Moore-Penrose inverse given by

$$\mathcal{I}_{\zeta}^+ = \Pi^+ \mathcal{I}_{\xi}^{-1} \Pi^{+'}, \quad \text{with} \quad \Pi^+ = \begin{pmatrix} M^+ & \mathbf{0} \\ \mathbf{0} & I \end{pmatrix},$$

such that the scaled innovation ε under Moore-Penrose inverse, denote ε_0 , is given by

$$\varepsilon_0 = \mathcal{I}_\zeta^+ \nabla_\zeta = \Pi^+ \mathcal{I}_\xi^{-1} \nabla_\xi \quad (15)$$

where we use $\nabla_\zeta = \Pi' \nabla_\xi$ and the fact that $\Pi^+ \Pi' = I$. The matrix M^+ in Π^+ is given by

$$M^+ = \text{diag} \left(M_1^+, M_2^+, \dots, M_n^+ \right), \quad M_i^+ = \left(\begin{array}{c} \frac{\partial \mu_i}{\partial \tau_i'} \\ \frac{\partial \omega_i}{\partial \tau_i'} \end{array} \right)^+, \quad i = 1, 2, \dots, n.$$

with the following expression for M_i^+

$$M_i^+ = \frac{1}{U'U \rho_i' \rho_i - (U' \rho_i)^2} J_i^{-1} \left[\begin{array}{c} \rho_i' \rho_i U' - \rho_i' U \rho_i' \\ \omega_i (\rho_i' U U' - U' U \rho_i') \end{array} \right]'. \quad (16)$$

This expression clarifies the reason behind the numerical instability for \mathcal{I}_ζ^+ . The random vector, U , can be proportional to (or nearly proportional to) ρ_i , (which has non-trivial probability). As the angle between U and ρ_i vanishes, the denominator vanishes to zero at a faster rate than the numerator, resulting in (arbitrarily) large elements of M_i^+ . To avoid this issue, we adopt the Tikhonov regularized Moore-Penrose inverse as our scaling matrix. The Tikhonov regularization involves a penalty term, $\lambda_i \geq 0$, for each assets, $i = 1, \dots, n$.

4.3.2 Tikhonov Regularized Moore-Penrose Inverse

Let $\boldsymbol{\lambda} = (\lambda_1, \dots, \lambda_n)'$ be a vector of non-negative penalty terms and define

$$M_{i,\lambda_i}^+ = M_i' (M_i M_i' + \lambda_i I_2)^+, \quad \text{where} \quad M_{i,\lambda_i}^+ = \text{argmin}_S \|SM_i - I_r\|_2 + \lambda_i \|S\|_2. \quad (17)$$

This is the Tikhonov regularized Moore-Penrose inverse where the boundary case, $\lambda_i = 0$, corresponds to the usual Moore-Penrose inverse in (16). The scaled innovation in (15) now can be adapted to

$$\varepsilon_\lambda = \Pi_\lambda^+ \mathcal{I}_\xi^{-1} \nabla_\xi, \quad (18)$$

where the Tikhonov regularized matrix Π_λ^+ is given by

$$\Pi_\lambda^+ = \left(\begin{array}{cc} M_\lambda^+ & \mathbf{0} \\ \mathbf{0} & I \end{array} \right), \quad \text{with} \quad M_\lambda^+ = \text{diag} \left(M_{1,\lambda_1}^+, M_{2,\lambda_2}^+, \dots, M_{n,\lambda_n}^+ \right).$$

Note that when $\boldsymbol{\lambda} = 0$, the scaled innovation $\varepsilon_{\boldsymbol{\lambda}}$ will return to ε_0 in (15).⁶

In our empirical analysis, we compare three definitions of ε , given by $\varepsilon_0 = \Pi^+ \mathcal{I}_{\xi}^{-1} \nabla_{\xi}$ (Moore-Penrose), $\varepsilon_{\boldsymbol{\lambda}} = \Pi_{\boldsymbol{\lambda}}^+ \mathcal{I}_{\xi}^{-1} \nabla_{\xi}$ (Tikhonov), and the very simple choice, $\varepsilon^* = \nabla_{\zeta}$ corresponding to $S = I$ with the identity as the scaling matrix. In specifications using $\varepsilon_{\boldsymbol{\lambda}}$, the vector of penalty parameters, $\boldsymbol{\lambda}$, is estimated and the empirical results clearly favors this choice for scaling matrix.

4.4 Decoupled Estimation

When n is large it becomes necessary to simplify the estimation problem further. This can be achieved by decoupling the dynamic structure for factor loadings from that of the idiosyncratic correlation matrix.

We propose an estimation strategy where the n score-driven models for ρ_i , $i = 1, \dots, n$ are estimated separately. These low-dimensional score-driven models yield the idiosyncratic residuals, $\hat{e}_{i,t}$, $i = 1, \dots, n$, that are subsequently used to estimate a score-driven model for the idiosyncratic correlation matrix C_e .

4.4.1 Decoupled Model for i -th Factor Loadings

To construct a score-driven model for the dynamic factor loading ρ_i using information from Z_i , we leverage the fact that the marginal distribution of a convolution- t distribution can be well approximated by a univariate Student's t distribution, see Patil (1965), Alcaraz López et al. (2023), and references therein. Here we will approximate the marginal distribution with the t -distribution that minimizes Kullback-Leibler divergence.

Therefore, we assume that

$$Z_i = \rho_i' U + \omega_i e_i, \quad e_i \simeq t_{\nu_i^*}^{\text{std}}(0, 1)$$

It is important to note that the approximating t -distribution, $t_{\nu_i^*}^{\text{std}}(0, 1)$, is only used to facilitate the construction of a score-driven model for ρ_i . Each of the score-driven models are estimated by maximizing the quasi log-likelihood function, defined by the approximating t -distribution, $t_{\nu_i^*}^{\text{std}}(\mu_i, \omega_i)$, where $\mu_i = \rho_i' U$ and $\omega_i = \sqrt{1 - \rho_i' \rho_i}$. The corresponding quasi log-likelihood function is given by

$$\ell^*(Z_i|U) = c_{\nu_i^*} - \log(\omega_i) - \frac{\nu_i^* + 1}{2} \log\left(1 + \frac{e_i^2}{\nu_i^* - 2}\right),$$

⁶One could also consider a regularization based on a common penalty parameter, $\lambda_i = \lambda^*$ for all $i = 1, 2, \dots, n$. We do not explore this in this paper.

where $c_{\nu_i^*}$ is a normalizing constant. From (18), Theorem 3 shows that the scaled score used to update the dynamics of $\tau(\rho_i)$ is given by

$$\varepsilon_{\lambda_i} = M_{i,\lambda_i}^+ \mathcal{I}_{\xi_i}^{-1} \nabla_{\xi_i}, \quad \text{where} \quad \nabla_{\xi_i} = \frac{\partial \ell(Z_i|U)}{\xi_i}, \quad \xi_i = (\mu_i, \omega_i)',$$

and M_{i,λ_i}^+ is defined in (17). Note that in this modeling strategy, the marginal densities of Z_i are approximated by a univariate Student's t -distribution with degrees of freedom ν_i^* . The parameter ν_i^* is estimated using a score-driven approach, which can be interpreted as minimizing the Kullback-Leibler (KL) divergence between the true marginal density function and the approximating density function.

Theorem 3. *Suppose that $e_i \sim t_{\nu_i^*}^{\text{std}}(0, 1)$ such that $Z_i|U \sim t_{\nu_i^*}^{\text{std}}(\mu_i, \omega_i^2)$ with $\mu_i = \rho_i' U$ and $\omega_i = \sqrt{1 - \rho_i' \rho_i}$, then the score vector and information matrix with respect to the dynamic parameter, $\tau(\rho_i)$, are given by*

$$\begin{aligned} \nabla_{\tau_i} &= J_i \left[\frac{W_i e_i}{\omega_i} U + \frac{1 - W_i e_i^2}{\omega_i^2} \rho_i \right] \\ \mathcal{I}_{\tau_i} &= J_i \left[\frac{(\nu_i^* + 1) \nu_i^*}{(\nu_i^* + 3)(\nu_i^* - 2)} \frac{U U'}{\omega_i^2} + \frac{2 \nu_i^*}{\nu_i^* + 3} \frac{1 - \omega_i^2}{\omega_i^4} \right] J_i \end{aligned}$$

where $W_i = \frac{\nu_i^* + 1}{\nu_i^* - 2 + e_i^2}$ and J_i is the Jacobian matrix $\partial \rho_i / \partial \tau_i$. With $\xi_i \equiv (\mu_i, \omega_i)'$, we have

$$\nabla_{\xi_i} = \frac{1}{\omega_i} \begin{pmatrix} W_i e_i \\ W_i e_i^2 - 1 \end{pmatrix}, \quad \mathcal{I}_{\xi_i} = \frac{1}{\omega_i^2} \begin{bmatrix} \frac{(\nu_i^* + 1) \nu_i^*}{(\nu_i^* + 3)(\nu_i^* - 2)} & 0 \\ 0 & \frac{2 \nu_i^*}{\nu_i^* + 3} \end{bmatrix},$$

such that the scaled score for updating the dynamics of τ_i is given by $\varepsilon_{\lambda_i} = M_{i,\lambda_i}^+ \mathcal{I}_{\xi_i}^{-1} \nabla_{\xi_i}$, where M_{i,λ_i}^+ is defined in (17).

4.4.2 Score-driven Model for Idiosyncratic Correlation Matrix C_e

The final stage of the decoupled estimation method is defined by a score-driven model for the idiosyncratic correlation matrix C_e using the estimated residuals $\hat{e} = (e_1, e_2, \dots, e_n)'$ from the first stage of decoupled estimation. Our distributional specifications are variants of the convolution t -distribution $e \sim \text{CT}_{m,\nu}^{\text{std}}(0, C_e^{1/2})$, and we consider four structure of C_e . (1) The most flexible structure is an Unrestricted Correlation matrix, which is heavily parameterized. A dynamic model for the elements in an unrestricted C_e is therefore only practical when the number of assets n is small. We estimate the model with $n = 12$ in our empirical analysis, but it will be difficult to increase the dimension much beyond 12. For larger dimensions we will need to impose structure on C_e . (2) The Block Correlation matrix for C_e offers a

way to reduce the number of free parameters, we will use subindustries to define the block structure. When the number of blocks is large (e.g. $K = 63$ which is used in some of our empirical analyses) additional structure is needed, and we consider two sparse variants that achieve this: (3) The Sparse Block Correlation matrix, which has idiosyncratic correlations for stocks in different sectors to be zero, and (4) Diagonal Block Correlation matrix for C_e , where the only nontrivial correlations are between stocks in the same subindustry.

The two sparse variants of C_e greatly simplify the estimation of the dynamic model for C_e , because it can be decomposed in to estimation involving subvectors of e that are specific to sectors or subindustries. For instance, with the Diagonal Block structure we have $C_e = \text{diag}(C_{[1,1]}, C_{[2,2]}, \dots, C_{[K,K]})$ where $C_{[k,k]}$ is an equicorrelation matrix with coefficient ϱ_{kk} . The unique element in $\log(C_{[k,k]})$, $\eta_k \in \mathbb{R}$, is given from (6), and it can be modeled as an unrestricted parameter. Let $e_{[k]}$ denote the corresponding subvector of e such that $\text{var}(e_{[k]}) = C_{[k,k]}$. These subvectors are independent for the Gaussian, HT, and CT distributions (provide that the cluster structure in CT is also based on subindustries such that $e_{(k)} \sim t_{n_k, \nu_k}^{\text{std}}(0, C_{[k,k]})$). This independence allows us to estimate the dynamics of η_k separately by using information from $e_{[k]}$ alone. The scaled score for updating η_k is then given by

$$\varepsilon_{[k]} = \mathcal{I}_{\eta_k}^{-1} \nabla_{\eta_k}, \quad \text{where} \quad \nabla_{\eta_k} = \frac{\partial \ell(e_{[k]})}{\eta_k}.$$

The formulas for the score ∇_{η_k} and the information matrix \mathcal{I}_{η_k} are provided in Theorem 4.

Theorem 4 (Multivariate- t with Equicorrelation Matrix C). *Suppose that $X \sim t_{n, \nu}^{\text{std}}(0, C)$, where C is an equicorrelation matrix with correlation coefficient ϱ . Then the score and information matrix with respect to dynamic parameter, $\eta = \frac{1}{n} \log\left(1 + n \frac{\varrho}{1-\varrho}\right)$, are given by*

$$\begin{aligned} \nabla_{\eta} &= -\frac{J}{2} \left[\frac{(n-1)}{1+(n-1)\varrho} - \frac{(n-1)}{1-\varrho} + W \left(\frac{X'X}{(1-\varrho)^2} - \frac{[1+(n-1)\varrho^2]X'\iota_n\iota_n'X}{(1-\varrho)^2[1+(n-1)\varrho]^2} \right) \right], \\ \mathcal{I}_{\eta} &= J^2 \left[\frac{1}{4} \frac{(3\phi-1)(n-1)^2}{(1+(n-1)\varrho)^2} + \frac{\phi}{2} \frac{(n-1)}{(1-\varrho)^2} + \frac{1-\phi}{4} \frac{(1-(n+1)\varrho)(n-1)^2}{(1+(n-1)\varrho)(1-\varrho)^2} \right], \end{aligned}$$

where $J = \frac{1}{(1-\varrho)(1+(n-1)\varrho)}$ and ι_n is a n -dimensional vector of ones, and

$$\phi = \frac{\nu+n}{\nu+n+2}, \quad W = \frac{\nu+n}{\nu-2+Q}, \quad Q = \frac{X'X}{1-\varrho} - \frac{\varrho X'\iota_n\iota_n'X}{(1-\varrho)[1+(n-1)\varrho]}.$$

When e follows the HT distribution, the subvectors $e_{[k]}$ are mutually independent and follow a HT distribution with ν_k degrees of freedom, where ν_k is the subvector of ν that corresponds to the k -th group. In this case, we can still estimate the dynamics of each of the η_k -vectors separately, solely using the information provided by $e_{[k]}$. The formulas for ∇_{η_k} and \mathcal{I}_{η_k} are provided in Theorem 5.

Theorem 5 (HT distribution with Equicorrelation Matrix C). *Suppose that $X \sim \text{CT}_{\mathbf{n}, \nu}^{\text{std}}(0, C^{1/2})$, where C is an equicorrelation matrix with correlation coefficient ϱ and $\mathbf{n} = \iota_n$. Then the score vector and information matrix with respect to the dynamic parameters, $\eta = \frac{1}{n} \log \left(1 + n \frac{\varrho}{1-\varrho} \right)$, are given by*

$$\begin{aligned} \nabla_{\eta} &= -\frac{J}{2} \left[\frac{(n-1)}{1+(n-1)\varrho} - \frac{(n-1)}{1-\varrho} \right] - \frac{J}{2} \sum_{i=1}^n W_i V_i \left[\frac{(nX_i - \iota'_n X)}{n(1-\varrho)^{3/2}} - \frac{(n-1)\iota'_n X}{n(1+(n-1)\varrho)^{3/2}} \right] \\ \mathcal{I}_{\eta} &= J^2 \left[\frac{1}{4} \frac{(n^2 + \mathcal{A}_1)(n-1)^2}{n^2(1+(n-1)\varrho)^2} + \frac{1}{4} \frac{(n-1)\mathcal{A}_2}{n^2(1-\varrho)^2} + \frac{1}{2} \frac{(n-1)^2 \mathcal{A}_3}{n^2(1+(n-1)\varrho)(1-\varrho)} \right] \end{aligned}$$

where J and ι_n are defined in Theorem 4, and

$$W_i = \frac{\nu_i + 1}{\nu_i - 2 + V_i^2}, \quad V_i = \frac{nX_i - \iota'_n X}{n\sqrt{1-\varrho}} + \frac{\iota'_n X}{n\sqrt{1+(n-1)\varrho}}$$

$\mathcal{A}_1 = 3\iota'_n \phi + (n-1)\iota'_n \psi - 2n$, $\mathcal{A}_2 = (3\iota'_n \phi - n)(n-1) + \iota'_n \psi + n$, $\mathcal{A}_3 = \iota'_n \psi + 2n - 3\iota'_n \phi$ where ϕ and ψ are both vectors with $\phi_i = \frac{\nu_i + 1}{\nu_i + 3}$, $\psi_i = \frac{\phi_i \nu_i}{\nu_i - 2}$ for $i = 1, 2, \dots, n$.

Under the sparse block structure where blocks are defined by subindustries, we can express $C_e = \text{diag}(C_{s_1}, C_{s_2}, \dots, C_{s_N})$ where C_{s_j} is a block correlation matrix of the j -th sector with group size s_j , for $j = 1, \dots, N$. From the formula (9), the unique element in $\log(C_{s_j})$ is $\eta_j \in \mathbb{R}^{s_j(s_j+1)/2}$, which can be modeled in an unrestricted way. Let $e_{\{j\}}$ denote the subvector of e that corresponds to the j -th sector, such that $e_{\{j\}} \sim (0, C_{s_j})$. When combined with either the Gaussian, CT, or HT distribution, $e_{\{j\}}$ will be mutually independent. This allows us to estimate the dynamics of η_j separately, using only the information from $e_{\{j\}}$. The scaled score for updating η_j is given by

$$\varepsilon_{\{j\}} = \mathcal{I}_{\eta_j}^{-1} \nabla_{\eta_j}, \quad \text{where} \quad \nabla_{\eta_j} = \frac{\partial \ell(e_{\{j\}})}{\eta_j}.$$

When e following CT or HT distribution, subvectors $e_{\{j\}}$ will also have a CT or HT distribution, $e_{\{j\}} \sim \text{CT}_{\mathbf{n}_j, \nu_j}^{\text{std}}(0, C_{s_1}^{1/2})$, with dimensions and degrees of freedom inherited from the parents distribution.

Note that this factorization is not feasible with the MT distribution, as its subvectors are not mutually independent. As a result, a score-driven model with the MT distribution cannot be estimated in this way, making it practical only in low-dimensional settings.

5 Empirical Analysis

5.1 Data

Our empirical analysis is based on daily close-to-close returns of constituents of the S&P 500 index and return series for each of the factor variables.⁷ Our sample period is from January 2007 to December 2023, with a total of $T = 4,278$ trading days.

5.1.1 Individual Returns series

The initial set of stocks consists of all stocks that were constituents of the S&P 500 index at some point during the sample period. We excluded stocks using the following exclusion criteria: (E1) stocks for which returns were not available over the full sample period; (E2) stocks from the Real Estate and Communication Services sectors, as is standard in the existing literature;⁸ (E3) stocks in sub-industries with fewer than 3 stocks (after applying E1 and E2). This resulted in a balanced sample with 323 stocks from 63 subindustries in 9 sectors. These are listed in Table 8 with ticker symbols under the 63 sub-industries in the Supplemental Material. We use the Global Industry Classification Standard (GICS) to sort stocks by their eight-digit GICS code in ascending order, and use sub-industries to define block structures in the idiosyncratic correlation matrix.

Before we analyze the full set of $n = 323$ stocks, which we refer to as the *Large Universe*, we will analyze a smaller subset with $n = 12$ stocks, which we label the *Small Universe*. The Small Universe provides a framework where it is possible to make comparisons with existing models. The simpler model also enables us to compare joint estimation of all model parameters with the two-stage method we use for the large universe.

5.1.2 Factor Variables

We use as many as $r = 15$ factors. These include those in the Fama-French five-factor model (FF5)⁹ and the momentum factor (UMD) by Carhart (1997). These six cross-sectional factors were obtained from the French (nd) Data Library. We also include nine sector-specific factors using returns for SPDR ETFs: Energy (XLE), Materials (XLB), Industrials (XLI),

⁷The data were obtained from the CRSP database of WRDS.

⁸The Real Estate sector was introduced as the 11th sector in 2016, and the Communication Services sector was introduced as an expanded and rebranded version of the Telecommunication Services sector. One consequence of this is that the corresponding sector-specific SPDR ETFs, (XLRE) and (XLC), are not available in the full sample period.

⁹FF5 represents the following portfolios: Market (MKT), small-minus-big (SMB), high-minus-low (HML), robust-minus-weak (RMW), and conservative-minus-aggressive (CMA).

Consumer Discretionary (XLY), Consumer Staples (XLP), Health Care (XLV), Financials (XLF), Information Technology (XLK), and Utilities (XLU), as in [Fan et al. \(2016\)](#), [Ait-Sahalia and Xiu \(2017\)](#), [Dai et al. \(2019\)](#), and [Bodilsen \(2024\)](#).

5.2 Standardized Asset Returns and Factor Variables

All model-specifications are based on the standardized variables, Z_t and F_t , that are obtained from $n + r$ univariate EGARCH models. These take the form

$$\begin{aligned} R_{i,t} &= a_{0,i} + a_{1,i}R_{i,t-1} + \sigma_{i,t}Z_{i,t}, & Z_{i,t} &\sim (0, 1), \\ \log \sigma_{i,t+1} &= b_{0,i} + b_{1,i} \log \sigma_{i,t} + b_{2,i}Z_{i,t} + b_{3,i}|Z_{i,t}|, \end{aligned} \quad (19)$$

for $i = 1, \dots, n$, which has an AR(1) structure for the conditional mean. The same univariate model is estimated for each of the r factor return series. Estimation results for the $n + r$ EGARCH models are reported in the Supplemental Material, see [Table B.1](#).

5.3 Small Universe

We begin by analyzing the Small Universe with $n = 12$ stocks and $r = 8$ factors. These stocks belong to four sub-industries (with three stocks in each) within the Health Care and Information Technology sectors (two sub-industries from each). The $r = 8$ factors are given by FF5, UMD, and the ETFs, XLV and XLK, that represent the two sector factors, Health Care and Information Technology, respectively.

The lower triangle of [Table 1](#) reports the full-sample unconditional correlation matrix and the upper triangle reports the idiosyncratic correlations. The block structures, as defined by sub-industries, are highlighted with shaded regions. The idiosyncratic correlations are based on the residuals obtained by regressing $Z_{i,t}$ on F_t and constant, $i = 1, \dots, n$.

Unconditional correlations are quite similar within each block of the correlation matrix. Two assets from the same subindustry are more correlated than stocks from different subindustries, albeit subindustries within the same sector are more correlated than subindustries from different sectors.

Correlations are greatly reduced by controlling for the eight factors. In fact, the idiosyncratic correlations involving stocks from different sectors are very close to zero. The average between-sectors idiosyncratic correlation is 0.012. The factor variables also explain much of the within-sector correlations, but to a lesser extent. In the Health Care sector, between-subindustries idiosyncratic correlations average about 0.056, whereas they average about 0.348 in the Information Technology sector. While these correlations are based on

Table 1: Unconditional and Idiosyncratic correlations (Small Universe)

	Health Care Distributors			Managed Health Care			Semiconductor Materials & Equipment			Semiconductors		
	ABC	CAH	MCK	HUM	UNH	WLP	AMAT	KLAC	LRCX	ADI	MCHP	TXN
ABC	1.000	0.472	0.520	0.044	0.058	0.080	0.013	0.021	0.015	0.033	0.001	0.012
CAH	0.640	1.000	0.497	0.025	0.034	0.062	0.043	0.044	0.040	0.038	0.013	0.006
MCK	0.669	0.655	1.000	0.063	0.068	0.074	0.012	0.001	0.012	-0.01	-0.02	-0.01
HUM	0.311	0.300	0.322	1.000	0.499	0.482	0.011	-0.01	0.005	-0.01	-0.02	-0.02
UNH	0.383	0.370	0.388	0.651	1.000	0.575	0.033	0.005	0.019	0.017	0.011	0.007
WLP	0.384	0.376	0.379	0.635	0.732	1.000	0.038	0.026	0.030	0.003	0.018	0.001
AMAT	0.260	0.301	0.264	0.215	0.285	0.276	1.000	0.539	0.613	0.351	0.369	0.329
KLAC	0.262	0.296	0.254	0.202	0.265	0.266	0.753	1.000	0.628	0.349	0.346	0.336
LRCX	0.254	0.290	0.256	0.205	0.269	0.264	0.790	0.794	1.000	0.354	0.358	0.344
ADI	0.291	0.317	0.271	0.221	0.297	0.277	0.663	0.653	0.651	1.000	0.520	0.540
MCHP	0.259	0.291	0.252	0.200	0.275	0.268	0.674	0.654	0.655	0.754	1.000	0.474
TXN	0.283	0.302	0.275	0.213	0.295	0.279	0.660	0.656	0.654	0.769	0.737	1.000

Note: Unconditional correlations for the 12 assets are reported below the diagonal, whereas the (crude) idiosyncratic correlations, based on the residuals obtained by regressing each asset return on the eight factor returns.

static factor loadings, the results do suggest that correlations can be non-negligible between subindustries in the same sector. The idiosyncratic correlations within subindustries are even larger and range from 47.2% to 62.8%. Thus, the eight factors, including the two sector factors, are clearly unable to explain the correlation structure between stocks in the same subindustry, at least not with static factor loadings.

The structure of the empirical idiosyncratic correlation matrix in Table 1 is the motivation for the sparse block correlation structures we introduced in Section 2.2.2. The results in Table 1 are based on a simplified structure with static factor loadings, and the dynamic factor correlation model may therefore reduce idiosyncratic correlations further. Next, we present the empirical results for the dynamic correlations model for the eight factor variables.

5.3.1 Correlation Matrix for Factor Variables

Table 2 reports the estimation results for the dynamic model for the eight factor variables in F_t . The correlation matrix in Panel A has correlations ranging from -30.7% to as much as 89.1%. The sector returns are highly correlated with market returns (and with each other).

Panel B of Table 2 presents the estimation results for the dynamic conditional correlation model for F_t , i.e. $C_{F,t}$ using the score-driven model for $\gamma_t^F = \text{vecl}(\log C_{F,t})$, by Tong et al. (2024). The maximized log-likelihood function and the corresponding BIC show that the

Table 2: Model for Dynamic Factor Variables (Small Universe)

Panel A: Unconditional Correlation Matrix C_F								
	MKT	SMB	HML	RMW	CMA	UMD	XLV	XLK
MKT	1.000	0.301	0.097	-0.295	-0.140	-0.057	0.766	0.891
SMB	0.301	1.000	0.113	-0.279	0.019	-0.129	0.136	0.165
HML	0.097	0.113	1.000	-0.064	0.500	-0.307	-0.051	-0.096
RMW	-0.295	-0.279	-0.064	1.000	0.093	0.014	-0.221	-0.228
CMA	-0.140	0.019	0.500	0.093	1.000	-0.050	-0.101	-0.268
UMD	-0.057	-0.129	-0.307	0.014	-0.050	1.000	0.001	0.032
XLV	0.766	0.136	-0.051	-0.221	-0.101	0.001	1.000	0.645
XLK	0.891	0.165	-0.096	-0.228	-0.268	0.032	0.645	1.000

Panel B: Estimation Results on Dynamic Correlations Models of C_F								
	$\bar{\mu}^F$	$\bar{\beta}^F$	$\bar{\alpha}^F$	$\bar{\nu}^F$	ν^F (range)	p	$-\ell(F)$	BIC
Gauss	0.086	0.985	0.031	∞		84	36967	74636
MT	0.088	0.986	0.032	10.30		85	36124	72959
HT	0.086	0.982	0.034	8.084	[6.259,11.43]	92	36254	73277

Note: Panel A reports the sample correlation matrix for the eight factors (FF5+UMD+XLV+XLK) and Panel B presents estimation results for score-driven models based on three distributional specifications. The vector of transformed correlations, $\gamma(C_F)$, has 28 elements and the average estimates of their score-model parameters, μ^F , α^F , β^F , and ν^F . The HT distribution has 8 degrees of freedom parameters and we report their range. The number of free parameters in each model is denoted by p , and we report the negative value of the log-likelihood function $\ell(F)$ for each model and the corresponding Bayesian Information Criterion (BIC), which is defined by $\text{BIC} = -2\ell + p \log T$. The largest log-likelihood and smallest BIC values are highlighted in bold font.

Table 3: Estimation Results for Factor Loadings (CT with Full Block C_e)

	Health Care Distributors			Managed Health Care			Semiconductor Materials & Equipment			Semiconductors		
	ABC	CAH	MCK	HUM	UNH	WLP	AMAT	KLAC	LRCX	ADI	MCHP	TXN
MKT	0.266	0.289	0.274	0.201	0.259	0.240	0.365	0.362	0.361	0.382	0.390	0.393
SMB	0.067	0.076	0.048	0.038	0.008	0.015	0.114	0.120	0.122	0.102	0.135	0.087
HML	0.005	0.044	0.028	0.038	0.043	0.070	-0.01	-0.02	-0.01	-0.01	-0.01	-0.02
RMW	0.007	-0.02	-0.01	0.000	0.013	-0.01	-0.08	-0.07	-0.08	-0.09	-0.08	-0.06
CMA	0.010	0.008	-0.01	-0.03	-0.03	0.005	-0.06	-0.05	-0.05	-0.04	-0.03	-0.01
UMD	0.013	-0.03	0.013	0.001	0.030	0.001	-0.02	0.001	-0.01	-0.02	-0.01	-0.01
XLV	0.426	0.429	0.416	0.400	0.482	0.452	0.189	0.192	0.184	0.228	0.202	0.224
XLK	0.144	0.176	0.160	0.120	0.156	0.143	0.459	0.455	0.437	0.465	0.468	0.487

Note: The averaged factor loadings for the model with Cluster- t distribution (CT) under Full Block C_e structure from Table 4.

heavy-tailed specifications, MT and HT, outperform the Gaussian specification, with MT (multivariate- t) having the best performance. That HT is inferior to MT, despite having more parameters, suggests that the nonlinear dependencies that a multivariate distribution implies is important for the factor variables. Consequently, we adopt the MT specification for F_t and use the corresponding $C_{F,t}$ to define the orthogonal factor variables, $U_t = C_{F,t}^{-1/2} F_t$, that are used in the subsequent analysis.

5.3.2 Factor Loadings and Idiosyncratic Correlations (joint estimation)

Next we turn to the central component of the model, which is the dynamic model of factor loadings and idiosyncratic correlations. We can estimate these components of the model in two ways: Either jointly (simultaneously) or decoupled. In this section we use joint estimation. These estimation results are presented in Table 4, where we report the average values of μ , α , β , ν , $\log \lambda$, as well as the individual estimates of ν_i and $\log \lambda_i$. Several interesting observations emerge from Table 4.

1. The heavy-tailed distributions offer substantial improvements over the Gaussian specification, as was the case in the model for F_t . But, here we find that the convolution- t distributions outperform the multivariate- t distribution with $\ell(Z|U)$ increases as much as 1,400 units.
2. The estimates of α (the updating-parameter in the score model) are larger for the heavy-tailed specifications than the Gaussian specification. We attribute this to the W -variables that mitigate the impact of extreme values (outliers). This is a well-

known feature of score-driven models, see e.g. [Harvey \(2013\)](#).

3. The CT specification has a cluster structure with fewer degrees of freedom and more nonlinear dependencies than the HT specification. While the estimated degrees of freedom in all CT specifications are quite similar to the average of the corresponding coefficients in the HT specifications, the largest log-likelihood (and best BIC) is achieved by the CT specification with the sparse block correlation structure. The additional degrees of freedom in the HT distribution cannot make up for the lack of nonlinear dependencies that the CT distribution can accommodate.
4. A comparison of specifications with different structures for the idiosyncratic correlation matrix, reveals that the diagonal structure (DBC) is too restrictive. This was also suggested by the preliminary empirical results in [Table 1](#), which were based on static factor loadings.
5. The penalty parameters, $\lambda_1, \dots, \lambda_n$ are all estimated to be large, which demonstrates a need to regularize the scaling matrix in the score model. The corresponding shocks are denoted ε_λ . The bottom of [Table 4](#) include comparisons with the score models use the Moore-Penrose inverse as scaling matrix (with shocks denoted ε_0 because $\lambda = 0$) and the simplistic $S = I$ scaling matrix, with shocks denoted ε^* . Using regularized model has the largest log-likelihood, $\ell(Z|U)$, in all cases. On average the regularized score driven model has a log-likelihood that is about 349 unit larger than the unregularized variant, ε_0 , and 375 units larger than the simplistic unscaled score model.

[Figure 3](#) illustrates the time series of block correlations for the specification estimated with Cluster- t distribution (CT) under Full Block C_e . The upper panels reveal sizable correlations for stocks in the same sector, especially for stocks in the same subindustry. The average correlation between the two Health Care subindustries, HCD and MHC, is just 0.056, but there is substantial time variation in this correlation that exceeds 0.20 on several occasions. This underscores the importance of permitting non-trivial idiosyncratic correlations to be time-varying. The lower panels in [Figure 3](#) present the estimated paths for correlations between stocks in different sectors. These are also close to zero and remain fairly constant over time. These observations support a sparse block correlation structure for C_e , which imposes idiosyncratic shocks from different sectors to be zero. This correlation structure, combined with the CT distributions has the smallest BIC.

[Table 3](#) presents the average factor loadings as estimated with the CT specification a block correlation structure for C_e . These are the average values of $\rho_{i,t}$ which related to U_t . The lower panel in [Table 3](#) presents the corresponding average loadings on the standardized

Table 4: Factor Loadings and Idiosyncratic Correlations (joint estimation)

	Unrestricted C_e				Full Block C_e				Sparse Block C_e				Diagonal Block C_e			
	Gauss	MT	CT	HT	Gauss	MT	CT	HT	Gauss	MT	CT	HT	Gauss	MT	CT	HT
$\bar{\mu}$	0.128	0.131	0.129	0.130	0.146	0.145	0.146	0.146	0.150	0.150	0.151	0.150	0.154	0.151	0.152	0.151
$\bar{\beta}$	0.949	0.942	0.951	0.950	0.924	0.963	0.937	0.959	0.948	0.936	0.938	0.952	0.946	0.953	0.939	0.961
$\bar{\alpha}$	0.010	0.016	0.016	0.018	0.014	0.020	0.028	0.027	0.015	0.025	0.029	0.028	0.016	0.024	0.026	0.027
$\bar{\nu}$	∞	4.874	3.764	3.449	∞	4.841	3.751	3.437	∞	4.850	3.755	3.441	∞	4.835	3.815	3.480
ν_1				3.675				3.624				3.632				3.661
ν_2			3.640	3.194			3.633	3.231			3.641	3.237		3.666		3.251
ν_3				3.312				3.279				3.281				3.296
ν_4				2.998				3.079				3.079				3.084
ν_5			3.710	3.867			3.719	3.673			3.722	3.667		3.729	3.672	
ν_6				3.570				3.549				3.544				3.548
ν_7				3.587				3.643				3.660				3.732
ν_8			3.782	3.113			3.733	3.289			3.735	3.304		3.801	3.361	
ν_9				3.707				3.510				3.513				3.488
ν_{10}				3.411				3.304				3.305				3.369
ν_{11}			3.925	3.240			3.918	3.295			3.923	3.298		4.064	3.466	
ν_{12}				3.715				3.768				3.771				3.833
$\log \bar{\lambda}$	5.744	3.121	2.937	3.035	5.639	3.555	3.431	3.344	5.913	3.685	3.234	4.501	6.228	3.827	4.576	3.974
$\log \lambda_1$	3.469	3.652	4.716	5.398	3.442	4.237	6.259	7.017	3.384	4.112	5.356	13.11	3.511	7.229	4.927	10.63
$\log \lambda_2$	9.574	4.165	3.753	6.445	10.37	8.421	9.987	7.854	11.23	9.323	7.170	11.49	13.48	8.017	10.85	8.133
$\log \lambda_3$	8.384	3.149	3.433	3.523	9.023	3.483	3.855	3.720	9.803	3.454	3.921	3.713	12.34	3.634	4.102	3.887
$\log \lambda_4$	9.817	6.419	8.099	9.049	10.27	9.782	8.841	9.371	11.17	9.896	9.745	13.26	10.66	8.556	19.02	10.06
$\log \lambda_5$	2.578	1.723	1.390	0.950	2.782	1.824	1.379	1.134	2.683	1.820	1.381	1.132	2.692	1.776	1.408	1.254
$\log \lambda_6$	4.958	4.482	3.369	3.223	5.157	4.220	3.503	3.400	5.133	4.172	3.561	3.444	4.897	4.274	3.627	3.682
$\log \lambda_7$	6.138	3.391	2.402	1.949	7.311	2.598	1.862	1.906	3.686	2.737	1.927	1.958	3.495	2.624	2.276	2.009
$\log \lambda_8$	9.702	3.134	2.666	0.660	10.62	1.568	0.636	0.375	11.50	2.000	0.727	0.418	12.53	1.815	1.009	0.735
$\log \lambda_9$	3.759	1.741	1.409	0.791	1.915	1.396	0.994	0.858	1.931	1.551	1.120	0.918	2.440	1.728	2.281	1.289
$\log \lambda_{10}$	2.558	1.056	0.868	1.429	1.882	1.019	0.820	1.572	1.875	1.080	0.837	1.610	2.055	1.567	1.672	2.476
$\log \lambda_{11}$	4.375	2.748	2.406	2.120	4.130	3.042	2.501	2.180	4.127	2.907	2.495	2.188	3.736	3.148	2.818	2.540
$\log \lambda_{12}$	3.614	1.798	0.732	0.879	4.355	1.072	0.535	0.741	4.423	1.165	0.544	0.759	2.882	1.554	0.908	0.987
p	498	499	502	510	330	331	334	342	318	319	322	330	312	313	316	324
$-\ell(Z U)$	50987	45891	44498	44455	51155	46059	44639	44657	51166	46073	44659	44671	51860	46827	45459	45547
BIC	106138	95954	93193	93174	105069	94886	92071	92174	104991	94813	92010	92101	106329	96271	93560	93803

Differences in $\ell(Z U)$ relative to $\varepsilon_\lambda = \Pi_\lambda^+ \mathcal{I}_\varepsilon^{-1} \nabla_\varepsilon$				
$\varepsilon^* = \nabla_\zeta$	-280	-330	-356	-367
$\varepsilon_0 = \mathcal{I}_\zeta^+ \nabla_\zeta$	-371	-286	-293	-302
	-294	-331	-358	-359
	-340	-287	-328	-298
	-294	-304	-341	-377
	-376	-292	-325	-309
	-447	-435	-437	-468

Note: Joint estimation results for the dynamic models of factor loadings and the idiosyncratic correlation matrix. We report the average values of μ , α , β , ν , $\log \lambda$, as well as the individual estimates of ν_i and $\log \lambda_i$. The number of model parameters is denoted by p , and we also report the negative log-likelihood function, $-\ell(Z|U)$, and the Bayesian Information Criterion (BIC). At the bottom, we compare the differences in $\ell(Z|U)$ with two alternative specifications for the scaled score, relative to the regularized version proposed in this paper. The largest log-likelihood and smallest BIC values for each structure of C_e are highlighted in bold font.

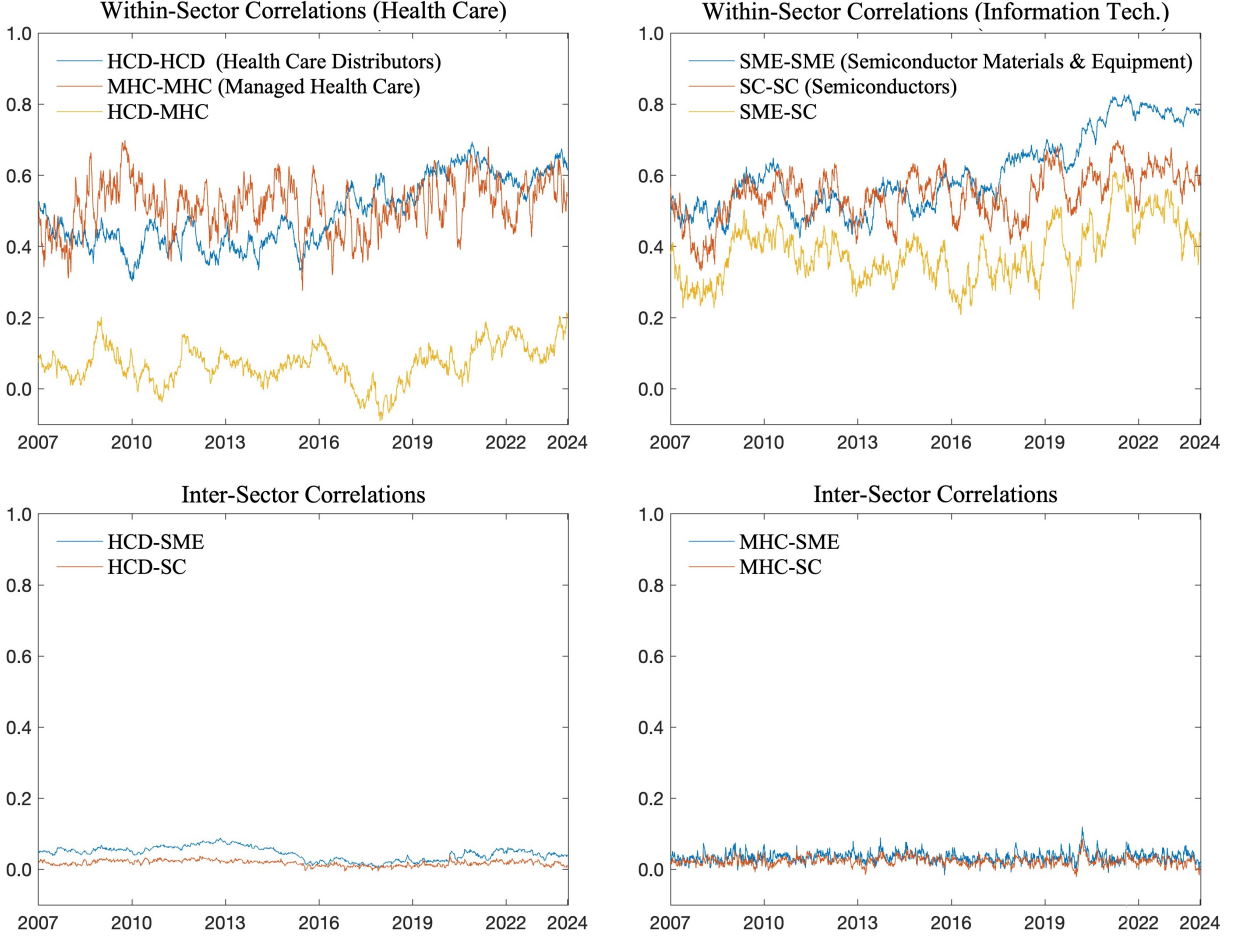


Figure 3: Time series of idiosyncratic block correlations among different sub-industries in small universe. The idiosyncratic correlations are based on the CT distribution with Full Block C_e in Table 4.

factor variables, F_t . The factor loadings for assets in the same sector tend to be quite similar, which is also reflected in the average factor loadings. The most significant factors are, not surprisingly, the market factor (MKT) and the two sector-factors (XLV and XLK). The size factor (SMB) is also important for the IT sector, but has small average impact on stocks in the Health Care sector.

Figure 4 displays the time series of factor loadings for Cencora Inc. (which has Ticker ABC). Its factor loadings, $\rho_{1,t}$, are estimated with the CT specification and the non-sparse block structure for C_e . The upper panels are the factor loadings for the six cross-sectional factors (FF5+UMD) and the lower left panel presents the factor loadings for the two sector-factors. The lower-right panel displays the fraction of the variance that is explained by factors, as defined by $\rho'_{1,t}\rho_{1,t}$. The factor loadings are time-varying and exhibit significant heterogeneity across different factors. From Table 3, although the average factor loading

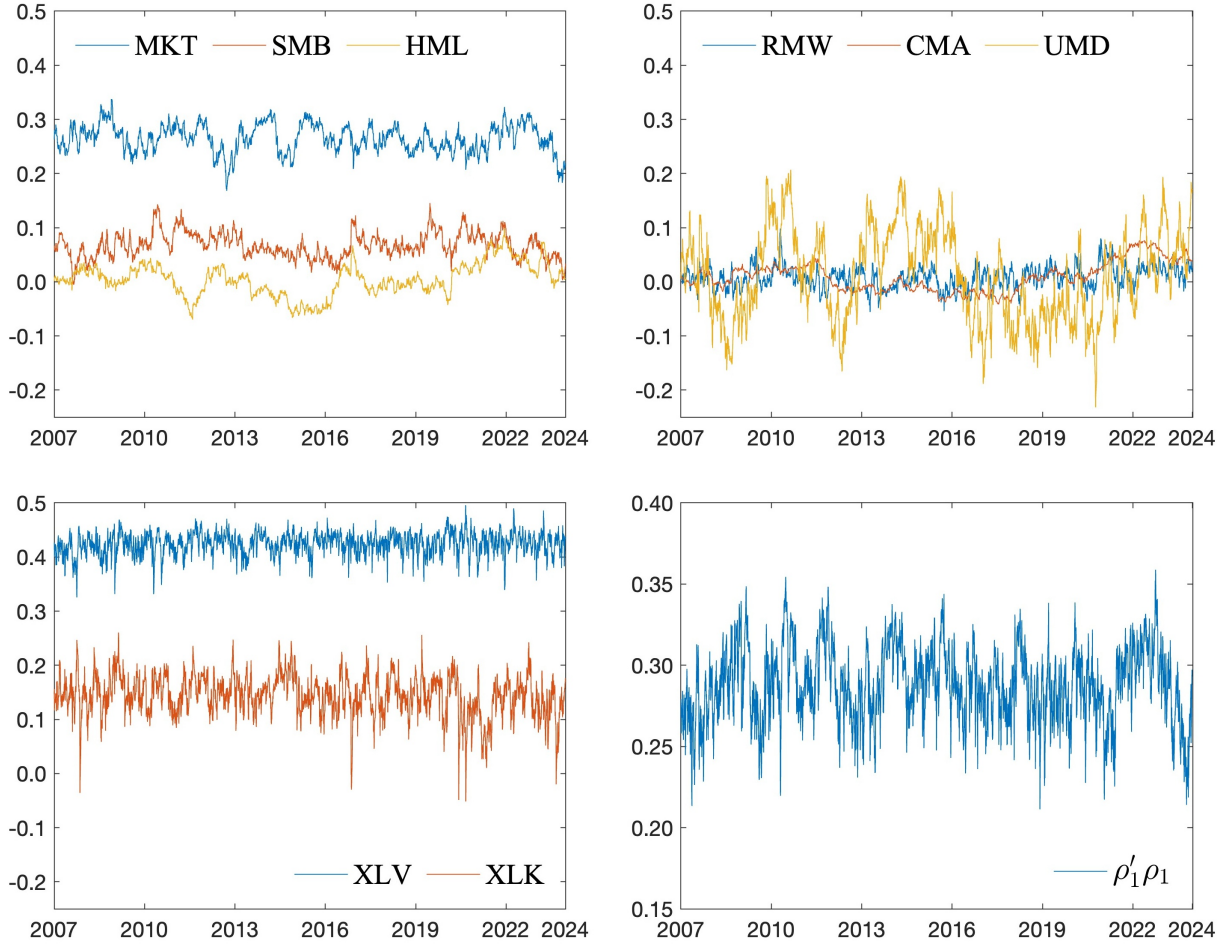


Figure 4: This figure displays the time series of Factor Loadings of Company ABC on eight factors (FF5+UMD+XLV+XLK). The final subfigure plots the dynamics of the explanatory power of the factors, measured by $\rho'_1 \rho_1$. The factor loadings are derived from the joint estimation results of the model with Full Block C_e under CT distribution in Table 4.

for HML is only 0.005, it dynamically ranges from -0.069 to 0.099 over time. Similarly, the factor loading on UMD (the momentum factor) displays the largest variation, despite having a mean of just 0.013. This stock belongs to the Health Care sector, and we also observe that its factor loading on XLV (Health care sector) is large and relatively stable over time. Additionally, there is a notable correlation with the Information Technology ETF (XLK), reflecting inter-sector dependencies. The last subfigure reveals that the averaged explanatory power of the factors is 0.288 and is also dynamic over time.

Table 5: Factor Loadings (decoupled estimation)

	Health Care Distributors			Managed Health Care			Semiconductor Materials & Equip.			Semiconductors		
	ABC	CAH	MCK	HUM	UNH	WLP	AMAT	KLAC	LRCX	ADI	MCHP	TXN
$\bar{\mu}$	0.140	0.130	0.124	0.096	0.137	0.125	0.136	0.134	0.131	0.149	0.157	0.158
$\bar{\beta}$	0.979	0.976	0.990	0.953	0.986	0.966	0.974	0.960	0.979	0.955	0.978	0.985
$\bar{\alpha}$	0.019	0.018	0.012	0.016	0.028	0.027	0.028	0.068	0.033	0.045	0.033	0.052
ν^*	3.702	3.332	3.368	3.145	3.728	3.766	3.978	3.468	3.832	3.644	3.623	4.001
$\log \lambda$	3.339	5.454	5.075	5.900	2.053	2.974	2.976	1.334	2.616	2.600	2.981	1.481
p	26	26	26	26	26	26	26	26	26	26	26	26
$-\ell(Z_i U)$	4784	4505	4683	4720	4637	4707	4294	4257	4439	4178	4064	4071
$\text{corr}(\rho)$	0.989	0.992	0.992	0.992	0.993	0.987	0.989	0.988	0.983	0.989	0.991	0.990

Note: Estimation results for the n factor loading models estimated with decoupled estimation, by maximizing $\ell(Z_i|U)$ for $i = 1, \dots, 12$, using the best-approximating t -distribution. We report the average values of μ , α , β , as well as the individual estimates of ν_i^* and $\log \lambda_i$. The number of model parameters is represented by p , and we report the negative log-likelihood function, $\ell(Z_i|U)$. The correlation between the factor loadings estimated with decoupled estimation and those obtained from joint estimation (using an unrestricted C_e with the HT distribution) are reported in the last row.

5.3.3 Decoupled Estimation

In this section, we estimate core component of our model with the decoupled estimation method as described in Section 4.4.1. The approach to estimation can be scaled to large dimensions, because the dynamic models for factor loadings are estimated separately for each asset and separately from the dynamic model for C_e . The dynamic models for the vector of factor loadings, ρ_i , is estimated by maximizing $\ell^*(Z_i|U)$, $i = 1, \dots, n$, from which we obtain the residuals, $e_t \in \mathbb{R}^n$, $t = 1, \dots, T$. These are subsequently used to estimated the dynamic model for the idiosyncratic correlation matrix, C_e , which is done by maximizing $\ell(e)$.

The results for the n factor loading models are reported in Table 5. The factor loading models are estimated by an approximating t -distribution, and the estimated degrees of freedom, ν_i^* , is small for all twelve assets, indicating that they all exhibit heavy tails.

While decoupled estimation is less efficient than joint estimation, it does yield quite similar paths for the estimated factor loadings. The empirical correlation between the two sets of factor loadings, denoted $\text{corr}(\rho)$, is reported in the last row of Table 5. The specification used for the joint estimation is that based on the HT distribution and an unrestricted C_e .

Table 6 presents the estimation results for the dynamic models of C_e , estimated with decoupled estimation by maximizing $\ell(e)$. We have estimated this model with four types

of distributions and four different correlation structures for C_e . Each of these models have the form of a Cluster-GARCH model, see [Tong et al. \(2024\)](#), and can be estimated as such. For some of the specifications with sparse C_e , it is possible to estimated lower-dimensional models for each sector/subindustry separated as discussed in [Section 4.4.2](#).

For instance with the Sparse-Block C_e we can estimate separate Cluster-GARCH models for the two sectors, with the exception of the case where the multivariate t -distribution is used (because it implies non-linear dependencies). Similarly with a diagonal block C_e , some of the specification can be simplified to (four) dynamic models with the structure detailed in [Theorem 4](#) and [Theorem 5](#). The estimated degrees of freedom are very similar to those we obtained with joint estimation.

The main difference between joint and decoupled estimation can be seen from the conditional log-likelihood of Z given F , which is given by $\ell(Z|U) = -\log |\Lambda_\rho| + \ell(e)$. While joint estimation maximizes this quantity, decoupled estimation only does so indirectly. This can be seen from the values of $\ell(Z|U)$ which are presented at the bottom of [Table 6](#). This log-likelihood is about 200 units smaller with decoupled estimation, which is to be expected because there are 300 fewer parameters being estimated when decoupled estimation is used. The last row of [Table 6](#) reports the correlation between the estimated elements of $C = \rho'\rho + \Lambda_\omega C_e \Lambda_\omega$, with joint estimation versus decouple estimation, and once again we do find very high correlations between the two estimation methods.

5.4 Out-of-Sample Results (Small Universe)

We next compare the estimated model specifications in terms of their out-of-sample (OOS) performance. We take the Z_t and U_t variables obtained from the full sample, and focus on the performance of the core model. We estimate each of the specification for the core correlation model with joint estimation and decoupled estimation, using 12 years of data (2007-2018). The estimated models are then compared out-of-sample using data from the years 2019 to 2023.

We report the out-of-sample results in [Table 7](#). The out-of-sample log-likelihood function, $\ell(Z|U)$, is reported for 32 model specifications, based on 4 different distributions, 4 different structures for the idiosyncratic correlation matrix, C_e , and the two estimation methods (joint and decoupled).

There are several interesting observations to be made from this out-of-sample comparison. First, the convolution- t distribution with a cluster structure, CT, is always the best distributional specification, regardless of the correlation structure and estimation method. This differs from the in-sample results where the HT specification (with an unrestricted C_e) had

Table 6: Decoupled Estimation for Dynamic Idiosyncratic Correlation Matrix

	Unrestricted C_e				Full Block C_e				Sparse Block C_e				Diagonal Block C_e			
	Gauss	MT	CT	HT	Gauss	MT	CT	HT	Gauss	MT	CT	HT	Gauss	MT	CT	HT
$\bar{\mu}$	0.112	0.118	0.114	0.110	0.174	0.207	0.210	0.476	0.285	0.331	0.345	0.476	0.374	0.461	0.476	0.476
$\bar{\beta}$	0.900	0.911	0.920	0.921	0.850	0.947	0.991	0.992	0.955	0.989	0.989	0.990	0.954	0.989	0.988	0.990
$\bar{\alpha}$	0.006	0.007	0.008	0.009	0.019	0.013	0.011	0.011	0.031	0.017	0.018	0.018	0.035	0.021	0.022	0.021
$\bar{\nu}$	∞	4.994	3.867	3.541	∞	4.972	3.862	3.535	∞	4.974	3.865	3.537	∞	4.899	3.887	3.549
ν_1				3.717				3.697				3.707				3.716
ν_2			3.672	3.192			3.655	3.230			3.662	3.235		3.672	3.236	3.236
ν_3			3.347	3.347			3.311	3.311			3.312	3.312		3.317	3.317	3.317
ν_4			3.041	3.041			3.117	3.117			3.116	3.116		3.119	3.119	3.119
ν_5			3.813	3.865			3.831	3.716			3.832	3.717		3.826	3.710	3.710
ν_6			3.926	3.671			3.651	3.651			3.654	3.654		3.644	3.644	3.644
ν_7				3.823			3.896	3.896			3.905	3.900		3.938	3.954	3.954
ν_8				3.317			3.406	3.406			3.407	3.407		3.429	3.429	3.429
ν_9				3.782			3.661	3.661			3.652	3.652		3.622	3.622	3.622
ν_{10}				3.520			3.426	3.426			3.424	3.424		3.439	3.439	3.439
ν_{11}			4.055	3.361			3.404	3.404			4.061	3.409		4.112	3.488	3.488
ν_{12}				3.855			3.906	3.906			3.908	3.908		3.916	3.916	3.916
p	198	199	202	210	30	31	34	42	18	19	22	30	12	13	16	24
$-\ell(e)$	64586	58771	57367	57289	64701	58955	57538	57508	64709	58968	57551	57520	65383	59656	58336	58334
BIC	130828	119206	116423	116334	129653	118169	115360	115367	129569	118095	115286	115291	130866	119421	116806	116869
$-\ell(Z U)_{\text{Seq}}$	51113	46154	44750	44672	51228	46338	44921	44891	51236	46351	44934	44903	51910	47039	45719	45717
$-\ell(Z U)_{\text{Joint}}$	50987	45891	44498	44455	51155	46059	44639	44657	51166	46073	44659	44671	51860	46827	45459	45547
corr(C)	0.991	0.992	0.994	0.994	0.986	0.991	0.994	0.994	0.987	0.992	0.994	0.995	0.988	0.990	0.993	0.994

Note: This table presents the second-step estimation results for the dynamic idiosyncratic correlation matrix C_e , obtained by maximizing $\ell(e)$, where e is filtered from the first-step estimation reported in Table 5. We report the average values of μ , α , β , and ν , as well as the individual estimates of ν_i . Additionally, we include the number of model parameters p , the negative log-likelihood function $\ell(e)$, and the Bayesian Information Criterion (BIC). The largest log-likelihood and smallest BIC values for each structure of C_e are highlighted in bold font. At the bottom of the table, we compute the log-likelihood values for returns, $\ell(Z|U) = -\log |\Lambda_\omega| + \ell(e)$, under joint and decoupled estimations, respectively, where Λ_ω in the decoupled estimation is taken from the first-step estimation in Table 5. Furthermore, we provide the correlation between the estimated elements of $C = \rho' \rho + \Lambda_\omega C_e \Lambda_\omega$, with joint estimation versus decouple estimation.

Table 7: Out-of-sample Results in Small Universe

	Gauss	MT	CT	HT
<i>Unrestricted C_e</i>				
Joint	-14040	-12592	-12288	-12303
Decoupled	-14049	-12613	-12291	-12312
<i>Full Block C_e</i>				
Joint	-14003	-12557	-12214	-12242
Decoupled	-14058	-12599	-12271	-12292
<i>Sparse Block C_e</i>				
Joint	-14014	-12551	-12202	-12230
Decoupled	-14055	-12598	-12241	-12256
<i>Diagonal Block C_e</i>				
Joint	-14289	-12900	-12602	-12603
Decoupled	-14299	-12854	-12545	-12582

Note: The out-of-sample log-likelihood $\ell(Z|U)$ is reported for different distributional specifications, different structures on the idiosyncratic correlation matrix, C_e , and the two estimation methods (joint and decoupled). The in-sample (estimation) period spans the years 2007 to 2018 and the out-of-sample (evaluation) period spans the years 2019 to 2023. The largest out-of-sample log-likelihood is highlighted in bold font.

the largest log-likelihood. Second, the Sparse Block structure for C_e tend to have the best out-of-sample performance followed by the (non-sparse) block correlation structure. The most restrictive structure, diagonal block correlation, has the worst out-of-sample performance, which is consistent with the in-sample results. Third, decoupled estimation is inferior to joint estimation, despite having much fewer parameters to estimate. The best out-of-sample log-likelihood is obtained with joint estimation of the model with the CT distribution and a sparse block correlation matrix. Overall, the out-of-sample results are in line with BIC statistics reported in Table 4.

5.5 Analysis of Large Universe

The large universe has $n = 323$ stocks that are distributed over 9 sectors and 63 subindustries. We use subindustries to define the block structure for the idiosyncratic correlation matrix, C_e , as we did in the small universe. The factor variables include the six cross-sectional factors (FF5+UMD) and the nine sector factors, such that this analysis is based on $r = 15$ factors.

The large number of stocks necessitates the use of decoupled estimation, as it is not practical to estimated the 232×15 dynamic factor loadings simultaneously in conjunction with a dynamic model for $C_e \in \mathbb{R}^{323 \times 323}$. We do not attempt to estimate a model for an

unrestricted C_e , because it has 52,003 distinct correlations. The block structure with $K = 63$ reduce this number to 2,016, which is also unpractically large. Instead we focus on the two sparse correlation structure for C_e : The sparse block correlation matrix, with 296 distinct correlations, and the diagonal block correlation matrix with 63 distinct correlations.

We do not consider the multivariate t -distribution (MT) in the large universe for two reasons. One is that it was found to be inferior to CT and HT in the Small Universe. More importantly, estimation with the MT distribution is far more involved than those for the three other distributions, because MT entails non-linear dependencies across subindustries. With decoupled estimation, the Gaussian, CT, and HT specifications, have simplified estimation of the dynamic idiosyncratic correlation matrix, because estimation can be done for each sector (or subindustry) separately. The reason is that the Gaussian and HT distributions are composed of independent elements, and the CT has a cluster structure that is aligned with subindustries.¹⁰

Figure 5 presents the sample block correlation matrix, C_e , based on the residuals from the 323 dynamic factor loading models. The correlation matrix is estimated using the method of moments by Archakov and Hansen (2024) with a 63×63 block structure based on subindustries. Solid lines are used to indicate the nine sectors and dashed lines are used to indicate the GICS Industries of which 42 are represented in the Large Universe. The names of the nine sectors are give along with their two-digit GICS code. For better visualization, we have truncated correlations smaller than 0.05 in absolute value to zero. There are many nontrivial correlations between subindustries, which renders the diagonal block correlation structure invalid. However, most non-trivial correlations are found between subindustries within the same sector, which is consistent with the sparse block correlation structure, which can also accommodate the heterogeneity in the correlations within and between subindustries. Most of large correlations between subindustries are for subindustries in the same industries (six-digit GICS codes). Two notable exceptions to this is the Material subindustry, “Fertilizers & Agricultural Chemicals”, which is correlated with several Energy subindustries, and the “Consumer Staples Merchandise Retail” subindustry, which is correlated with subindustries in the Consumer Discretionary sector, primarily those in the “Consumer Discretionary Distribution & Retail” industry group (2550).

The results in Figure 5 was based on a static block correlation matrix. We present the results for the dynamic model for C_e in Table 8 for each of the nine sectors. For each sector, we report the average estimates of μ , α , β , and ν , as well as the range of the estimates for ν_i (the degrees of freedom parameters). We also report the number of model parameters, p ,

¹⁰The computationally most complex structure is that for the sector “Industrials” which has 11 subindustries, which is manageable.

in each sector model, the negative log-likelihood function, $-\ell(e_{\{j\}})$, and the corresponding Bayesian Information Criterion (BIC). The largest log-likelihood and the smallest BIC are highlighted in bold font for each sector, and the best model specification is. The best model specification is in all cases provided by the HT distribution with the Sparse Block Correlation structure. The latter confirms the need to account for correlations between subindustries in the same sector, as was indicated by the static sample correlations in Figure 5. We note that the estimate of $\bar{\mu}$ is smaller in the specifications with Sparse Block structure, relative to Diagonal Block structure, which is consistent with within-subindustry correlations tend to be much larger than between-subindustry correlations.

Figure 6 presents the time series of various correlations derived from the dynamic idiosyncratic correlation matrix C_e in large universe, estimated with a sparse block correlation matrix, C_e , and the HT distribution. Most non-trivial idiosyncratic correlations are for subindustries in the same industry, see Figure 5. So, for nine industries (one from each sector) we selected a pair of subindustries. Their time series of within-subindustry and between-subindustries correlations are displayed in Figure 6. Many of these time series have strong and persistent variation and can find a very evident time varying pattern in each subfigures, which means it is very important to consider the dynamics in idiosyncratic correlation matrix C_e .

Table 9 conduct the out-of-sample analysis. As the same in small universe, we estimate all models using data from 2007 to 2018 and evaluate the estimated models using out-of-sample data from 2019 to 2023. The out-of-sample results are largely consistent with the in-sample results. The HT distribution with a sparse block structure for C_e provides the best performance in all sectors, with the exception of the Energy sector where CT (which permits nonlinear dependencies with subindustries) outperform the HT distribution. The out-of-sample results show that the in-sample results in Table 8 are not driven by overfitting.

6 Conclusion

In this paper, we introduced a novel dynamic factor correlation model with a variation-free parametrization of factor loadings. To the best of our knowledge, this is the first multivariate GARCH model that simultaneously can accommodate dynamic factor structures, time-varying, heavy-tailed distributions, and dependent idiosyncratic shocks with time-varying correlations. The proposed framework incorporates a score-driven approach to jointly estimate dynamic factor loadings and the idiosyncratic correlation matrix. A decoupled estimation strategy make it possible to scale the model to high dimensions, as illustrated in our empirical application. Our novel parametrization of factor loadings facilitates simple

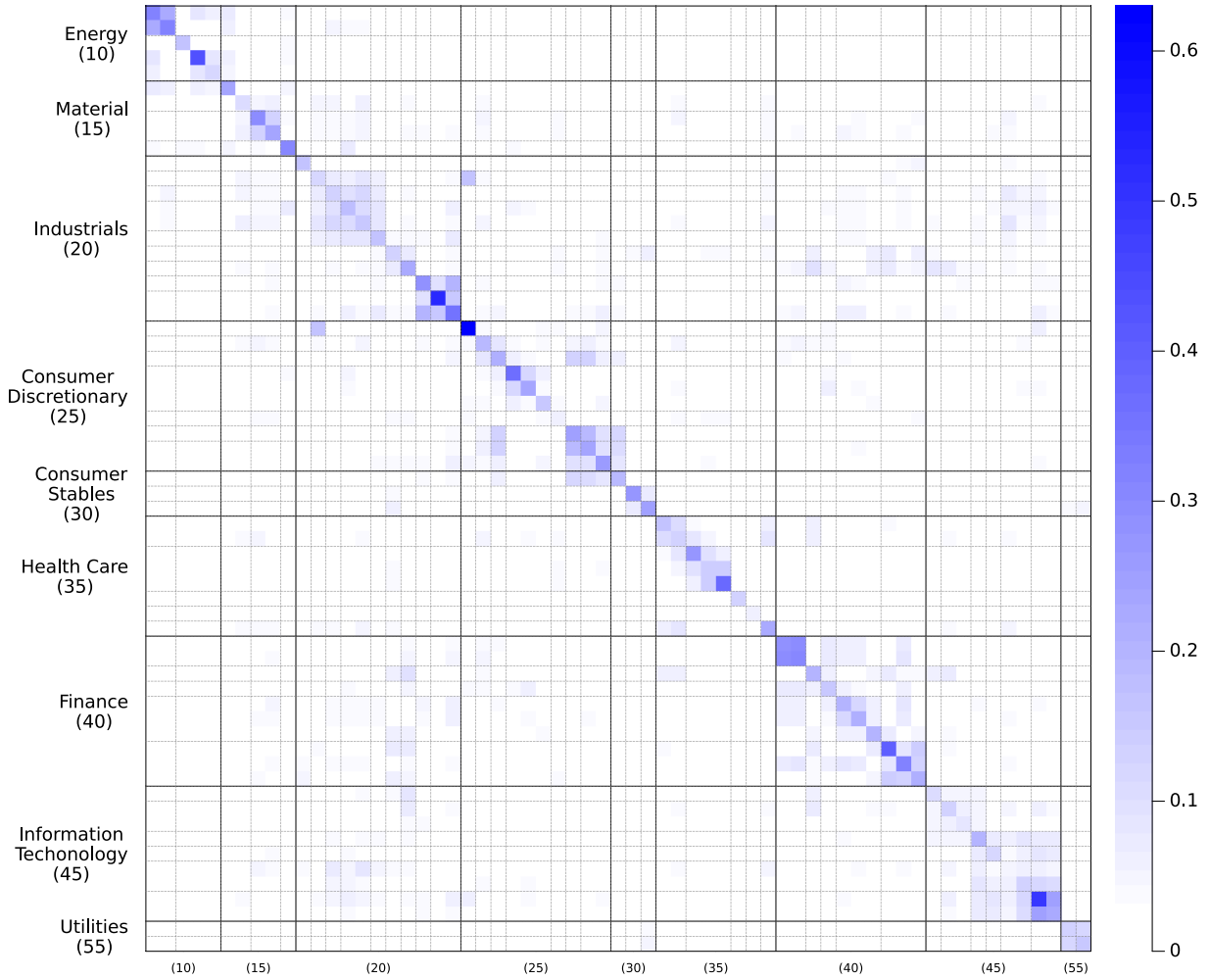


Figure 5: The sample estimate of C_e with a block structure defined by subindustry. The nine sectors are indicated with the black lines and industries are indicated with dashed lines. The block correlation matrix is estimated from the residuals, $\hat{\epsilon}_t$, using the method of Archakov and Hansen (2024). For better visualization, correlations smaller than 0.05 in absolute value are truncated to zero.

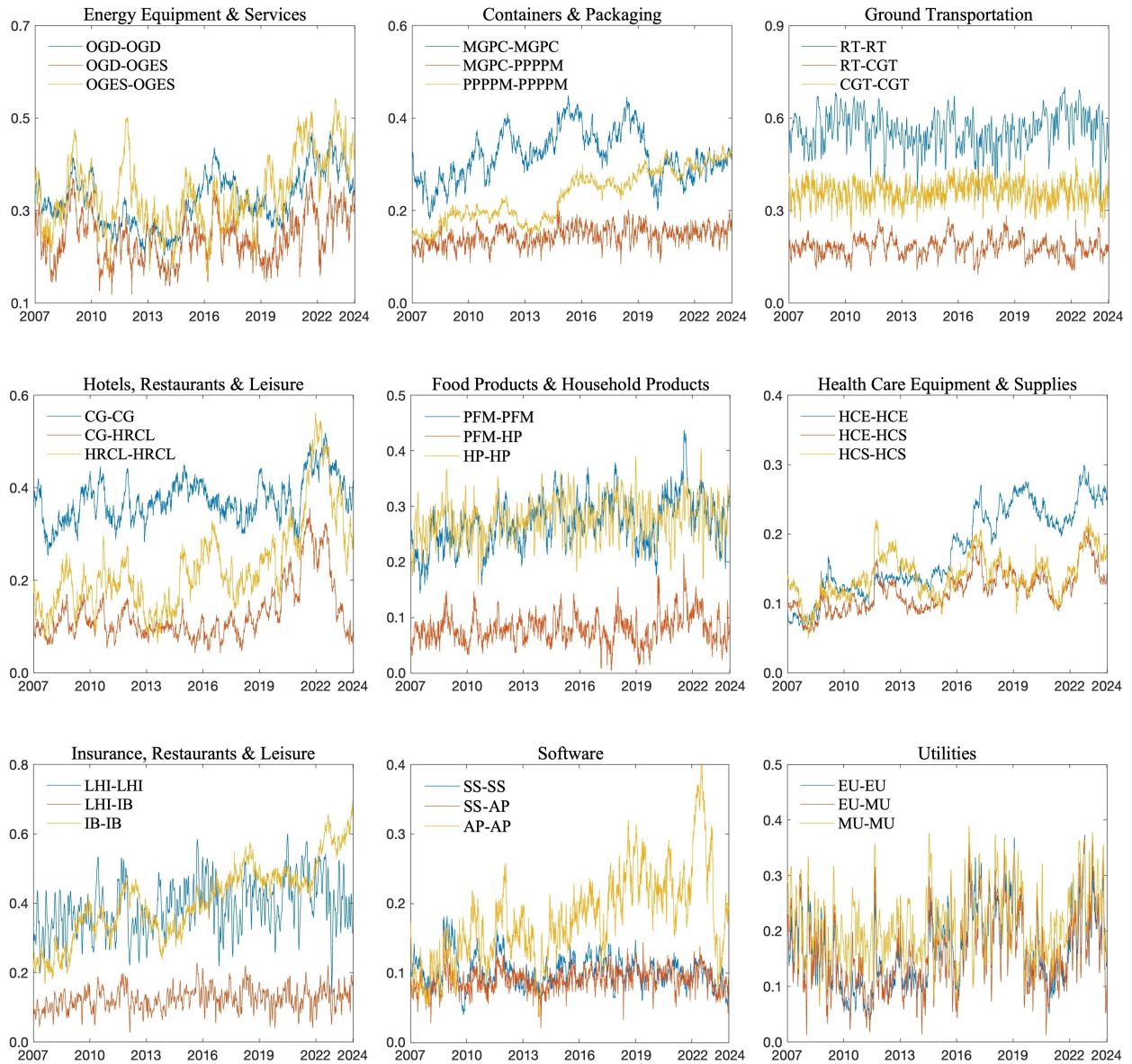


Figure 6: Some time series for the idiosyncratic correlations in the large universe, estimated with a sparse block structure and the HT distribution. For nine industries (four digits) we selected a pair of subindustries, and present their within- and between-subindustry correlations. Subindustries are labeled with the first letters in their names (e.g. “OGD” refers to the “Oil & Gas Drilling” subindustry).

imposition of sparsity constraints and simplifies the dynamic modeling of these.

The empirical applications demonstrate the flexibility and effectiveness of the proposed model. The analysis of a small universe with 12 assets allowed for comparisons across different specifications and estimation methods, revealing the advantages of a convolution- t distribution with a block structure in the idiosyncratic correlation matrix. Our large universe application involve 323 assets from the S&P 500 and it demonstrate the scalability of the model. The empirical results underscored the importance of permitting some dependence in the idiosyncratic correlation matrix. We found that the sparse block structure – partitioned by sectors and subindustries – provides the best fit according to likelihood-based criteria. Similarly, we found that Convolution- t distributions outperform the standard specifications with Gaussian and multivariate t -distributions. There was strong evidence for time variation in the factor loadings, which can explain dynamic shifts in asset return dependencies. The empirical evidence for nontrivial correlation between idiosyncratic shocks is strong, but the nontrivial correlations are primarily found between stocks in the same sector. These observations a consistent with the structure of a sparse block correlation matrix, which was also the structure that had the best out-of-sample performance in all comparisons.

References

- Ait-Sahalia, Y. and Xiu, D. (2017). Using principal component analysis to estimate a high dimensional factor model with high-frequency data. *Journal of Econometrics*, 201(2):384–399.
- Alcaraz López, O. L., Garcia Fernández, E. M., Latva-aho, M., et al. (2023). Fitting the distribution of linear combinations of variables with more than 2 degrees of freedom. *Journal of Probability and Statistics*, 2023:9967290.
- Andreou, E., Gagliardini, P., Ghysels, E., and Rubin, M. (2024). Spanning latent and observable factors. *Journal of Econometrics*, page 105743.
- Archakov, I. and Hansen, P. R. (2021). A new parametrization of correlation matrices. *Econometrica*, 89:1699–1715.
- Archakov, I. and Hansen, P. R. (2024). A canonical representation of block matrices with applications to covariance and correlation matrices. *Review of Economics and Statistics*, 106:1–15.
- Archakov, I., Hansen, P. R., and Lunde, A. (2025). A multivariate Realized GARCH model. *Journal of Econometrics*, forthcoming.

- Bodilsen, S. T. (2024). Large-dimensional portfolio selection with a high-frequency-based dynamic factor model. *Journal of Financial Econometrics*, page nbae018.
- Bollerslev, T. (1986). Generalized autoregressive heteroskedasticity. *Journal of Econometrics*, 31:307–327.
- Carhart, M. M. (1997). On persistence in mutual fund performance. *Journal of Finance*, 52:57–82.
- Creal, D., Koopman, S. J., and Lucas, A. (2011). A dynamic multivariate heavy-tailed model for time-varying volatilities and correlations. *Journal of Business and Economic Statistics*, 29:552–563.
- Creal, D., Koopman, S. J., and Lucas, A. (2013). Generalized autoregressive score models with applications. *Journal of Applied Econometrics*, 28:777–795.
- Creal, D. and Tsay, R. S. (2015). High dimensional dynamic stochastic copula models. *Journal of Econometrics*, 189:335–345.
- Dai, C., Lu, K., and Xiu, D. (2019). Knowing factors or factor loadings, or neither? evaluating estimators of large covariance matrices with noisy and asynchronous data. *Journal of Econometrics*, 208:43–79.
- Darolles, S., Francq, C., and Laurent, S. (2018). Asymptotics of Cholesky GARCH models and time-varying conditional betas. *Journal of Econometrics*, 204:223–247.
- Engle, R. and Kelly, B. (2012). Dynamic equicorrelation. *Journal of Business and Economic Statistics*, 30:212–228.
- Engle, R. and Kroner, K. (1995). Multivariate simultaneous generalized ARCH. *Econometric theory*, 11:122–150.
- Engle, R. F. (1982). Autoregressive conditional heteroskedasticity with estimates of the variance of U.K. inflation. *Econometrica*, 45:987–1007.
- Engle, R. F. (2002). Dynamic conditional correlation: A simple class of multivariate generalized autoregressive conditional heteroskedasticity models. *Journal of Business and Economic Statistics*, 20:339–350.
- Engle, R. F. (2016). Dynamic conditional beta. *Journal of Financial Econometrics*, 14(4):643–667.

- Fan, J., Furger, A., and Xiu, D. (2016). Incorporating global industrial classification standard into portfolio allocation: A simple factor-based large covariance matrix estimator with high-frequency data. *Journal of Business and Economic Statistics*, 34:489–503.
- French, K. R. (n.d.). Data library. Accessed: 2024-09-20.
- Hansen, P. R. and Lunde, A. (2005). A forecast comparison of volatility models: Does anything beat a GARCH(1,1)? *Journal of Applied Econometrics*, 20:873–889.
- Hansen, P. R., Lunde, A., and Voev, V. (2014). Realized beta GARCH: A multivariate GARCH model with realized measures of volatility. *Journal of Applied Econometrics*, 29:774–799.
- Hansen, P. R. and Tong, C. (2024). Convolution- t distributions. *arXiv:2404.00864*, [econ.EM].
- Harvey, A. (2013). *Dynamic Models for Volatility and Heavy Tails: with Applications to Financial and Economic Time Series*. Cambridge University Press.
- Linton, O. and McCrorie, J. R. (1995). Differentiation of an exponential matrix function: Solution. *Econometric Theory*, 11:1182–1185.
- Nelson, D. B. (1991). Conditional heteroskedasticity in asset returns: A new approach. *Econometrica*, 59:347–370.
- Oh, D. H. and Patton, A. J. (2017). Modeling dependence in high dimensions with factor copulas. *Journal of Business and Economic Statistics*, 35:139–154.
- Oh, D. H. and Patton, A. J. (2018). Time-varying systemic risk: Evidence from a dynamic copula model of cds spreads. *Journal of Business and Economic Statistics*, 36:181–195.
- Oh, D. H. and Patton, A. J. (2023). Dynamic factor copula models with estimated cluster assignments. *Journal of Econometrics*, 237. 105374.
- Opschoor, A., Lucas, A., Barra, I., and van Dijk, D. (2021). Closed-form multi-factor copula models with observation-driven dynamic factor loadings. *Journal of Business and Economic Statistics*, 39:1066–1079.
- Patil, V. H. (1965). Approximation to the Behrens-Fisher distributions. *Biometrika*, 52:267–271.
- Sheppard, K. and Xu, W. (2019). Factor high-frequency-based volatility (HEAVY) models. *Journal of Financial Econometrics*, 17:33–65.

Tong, C. and Hansen, P. R. (2023). Characterizing correlation matrices that admit a clustered factor representation. *Economic Letters*, 233. 111433.

Tong, C., Hansen, P. R., and Archakov, I. (2024). Cluster GARCH. *arXiv:2406.06860*, [econ.EM].

Table 8: Estimation Results (Large Universe)

	$\bar{\mu}$	$\bar{\beta}$	$\bar{\alpha}$	$\bar{\nu}$	ν_{\min}	ν_{\max}	p	$-\ell(e)$	BIC
Energy Sector (10)									
<i>Sparse Block C_e</i>									
Gauss	0.095	0.845	0.018				45	98096	196569
CT	0.103	0.883	0.016	5.360	4.387	6.232	50	93065	186548
HT	0.103	0.880	0.015	4.741	3.511	6.915	62	92892	186302
<i>Diagonal Block C_e</i>									
Gauss	0.222	0.994	0.012				15	98792	197709
CT	0.255	0.993	0.016	5.368	4.383	6.196	20	93821	187809
HT	0.249	0.994	0.014	4.746	3.559	6.997	30	93674	187599
Materials Sector (15)									
<i>Sparse Block C_e</i>									
Gauss	0.082	0.800	0.025				45	146905	294186
CT	0.082	0.807	0.023	4.406	3.792	5.136	50	134784	269985
HT	0.082	0.855	0.021	3.704	2.899	5.131	70	133168	266921
<i>Diagonal Block C_e</i>									
Gauss	0.163	0.939	0.019				15	147415	294955
CT	0.208	0.958	0.026	4.416	3.823	5.148	20	135351	270868
HT	0.196	0.975	0.020	3.705	2.892	5.171	30	133787	267825
Industrials Sector (20)									
<i>Sparse Block C_e</i>									
Gauss	0.044	0.834	0.014				198	310906	623467
CT	0.048	0.860	0.013	4.211	3.474	5.010	209	282381	566509
HT	0.048	0.833	0.016	3.612	2.832	4.397	251	279157	560412
<i>Diagonal Block C_e</i>									
Gauss	0.184	0.839	0.029				33	313656	627588
CT	0.220	0.956	0.028	4.240	3.499	5.051	44	285484	571336
HT	0.210	0.889	0.035	3.614	2.829	4.495	121	282542	566096
Consumer Discretionary Sector (25)									
<i>Sparse Block C_e</i>									
Gauss	0.048	0.848	0.013				165	268484	538348
CT	0.054	0.881	0.011	3.939	3.145	4.939	175	238769	479001
HT	0.054	0.858	0.013	3.474	2.514	6.319	212	236154	474080
<i>Diagonal Block C_e</i>									
Gauss	0.177	0.906	0.021				30	270545	541341
CT	0.222	0.968	0.021	3.968	3.155	4.935	40	241168	482671
HT	0.209	0.962	0.029	3.500	2.507	6.311	90	238843	478439
Consumer Staples Sector (30)									
<i>Sparse Block C_e</i>									
Gauss	0.096	0.770	0.029				18	93581	187313
CT	0.102	0.902	0.026	4.054	3.889	4.220	21	84125	168426
HT	0.102	0.909	0.026	3.367	3.090	4.035	34	83085	166455
<i>Diagonal Block C_e</i>									
Gauss	0.183	0.875	0.030				9	93710	187495
CT	0.196	0.898	0.029	4.045	3.884	4.193	12	84225	168550
HT	0.185	0.918	0.025	3.355	3.092	3.922	21	83225	166626

Note: Table continued on next page.

Table 8: (cont.)

	$\bar{\mu}$	$\bar{\beta}$	$\bar{\alpha}$	$\bar{\nu}$	ν_{\min}	ν_{\max}	p	$-\ell(e)$	BIC
Health Care Sector (35)									
<i>Sparse Block C_e</i>									
Gauss	0.038	0.866	0.015				108	275826	552554
CT	0.036	0.914	0.013	3.964	3.400	4.420	116	246629	494228
HT	0.036	0.921	0.011	3.318	2.511	4.264	155	242199	485695
<i>Diagonal Block C_e</i>									
Gauss	0.139	0.910	0.024				24	277265	554730
CT	0.137	0.966	0.021	3.990	3.458	4.443	32	248323	496913
HT	0.129	0.957	0.021	3.340	2.518	4.212	88	244037	488811
Financial Sector (40)									
<i>Sparse Block C_e</i>									
Gauss	0.042	0.937	0.012				165	316545	634470
CT	0.045	0.922	0.016	4.536	3.671	5.272	175	289209	579880
HT	0.045	0.919	0.019	3.935	3.014	6.127	220	287231	576301
<i>Diagonal Block C_e</i>									
Gauss	0.166	0.939	0.033				30	320172	640594
CT	0.184	0.968	0.036	4.498	3.693	5.063	40	293115	586564
HT	0.171	0.957	0.041	3.842	3.005	5.589	90	291676	584105
Information Technology Sector (45)									
<i>Sparse Block C_e</i>									
Gauss	0.041	0.830	0.014				135	269981	541091
CT	0.043	0.868	0.011	3.810	3.122	4.942	144	238939	479083
HT	0.043	0.899	0.011	3.282	2.658	4.981	181	233593	468699
<i>Diagonal Block C_e</i>									
Gauss	0.119	0.949	0.012				27	272230	544687
CT	0.146	0.979	0.015	3.842	3.186	4.953	36	241795	483892
HT	0.137	0.968	0.017	3.288	2.655	4.702	72	236975	474552
Utilities Sector (55)									
<i>Sparse Block C_e</i>									
Gauss	0.084	0.921	0.036				9	100548	201171
CT	0.091	0.975	0.035	6.969	6.958	6.979	11	96396	192884
HT	0.091	0.945	0.053	5.370	4.293	6.761	26	96080	192377
<i>Diagonal Block C_e</i>									
Gauss	0.109	0.940	0.029				6	101197	202444
CT	0.118	0.971	0.042	6.878	6.877	6.879	8	97045	194157
HT	0.122	0.954	0.057	5.299	4.158	6.721	24	96871	193943

Note: The estimation results for the dynamic idiosyncratic correlation matrix C_e in the large universe, obtained by maximizing $\ell(e)$. For each of the nine sectors. We report the average values of μ , α , β , and ν , as well as the range of the estimates of degrees of freedom. Additionally, the number of model parameters p , the negative log-likelihood function $\ell(e_{\{j\}})$, and the Bayesian Information Criterion (BIC) are included. The largest log-likelihood and smallest BIC values for each structure of C_e are highlighted in bold font.

Table 9: Out-of-sample Results in Large Universe

Sector	Sparse Block C_e			Diagonal Block C_e		
	Gauss	CT	HT	Gauss	CT	HT
Energy	-28378	-26851	-26884	-28584	-27103	-27132
Materials	-43471	-39734	-39498	-43584	-39887	-39655
Industrials	-90031	-81666	-81301	-90841	-82591	-82314
Consumer Discretionary	-77730	-69497	-69267	-78353	-70282	-70070
Consumer Staples	-28190	-24983	-24798	-28247	-25032	-24863
Health Care	-81218	-71819	-71037	-81477	-72216	-71450
Financial	-93339	-83056	-82745	-94066	-84246	-84125
Information Technology	-76309	-66810	-65709	-77112	-67784	-66846
Utilities	-29539	-28252	-28200	-29771	-28540	-28498

Note: Out-of-sample log-likelihoods, $\ell(e)$, for for six model-specifications (three distributions and two structures for C_e) for each of the nine sectors. In-sample estimation is based on data from 2007 to 2018 and the out-of-sample period spans the five years, from 2019 to 2023. The largest log-likelihood in each row is highlighted in bold font.

A Appendix of Proofs

A Novel Parametrization of Factor Loadings

Proof of Theorem 1. Let $C^* = \text{cor}((Z_i, U)')$, then $C^* = I + H$ where

$$H = \begin{bmatrix} 0 & \rho'_i \\ \rho_i & 0 \end{bmatrix} \in \mathbb{R}^{(r+1) \times (r+1)}.$$

Since the largest eigenvalue of $H'H$ is $\rho'_i\rho_i$, we have the following expression for the matrix logarithm

$$\log(C^*) = \sum_{k=1}^{\infty} (-1)^{k+1} \frac{H^k}{k} = - \sum_{k=1}^{\infty} \frac{H^{2k}}{2k} + \sum_{k=1}^{\infty} \frac{H^{2k-1}}{2k-1},$$

where

$$H^{2k} = \begin{bmatrix} (\rho'_i\rho_i)^k & 0 \\ 0 & (\rho_i\rho'_i)^k \end{bmatrix} \quad \text{and} \quad H^{2k-1} = \begin{bmatrix} 0 & (\rho'_i\rho_i)^{k-1}\rho'_i \\ \rho_i(\rho'_i\rho_i)^{k-1} & 0 \end{bmatrix}.$$

So, the diagonal blocks of $\log(C^*)$ are given by $-\sum_{k=1}^{\infty} \frac{1}{2k} (\rho'_i\rho_i)^k = \frac{1}{2} \log(1 - \rho'_i\rho_i) \in \mathbb{R}$ and

$$-\sum_{k=1}^{\infty} \frac{1}{2k} (\rho_i\rho'_i)^k = -\frac{1}{2\rho'_i\rho_i} \left[\sum_{k=1}^{\infty} \frac{1}{k} (\rho_i\rho'_i)^k \right] (\rho\rho') = \frac{\log(1 - \rho'_i\rho_i)}{2\rho'_i\rho_i} (\rho_i\rho'_i) \in \mathbb{R}^{r \times r}.$$

The off-diagonal blocks are zero if $\rho'_i\rho_i = 0$. Otherwise, if $\rho'_i\rho_i \neq 0$, we have

$$\begin{aligned} \tau'_i &= \sum_{k=1}^{\infty} \frac{(\rho'_i\rho_i)^{k-1}}{2k-1} \rho'_i = \frac{1}{\sqrt{\rho'_i\rho_i}} \left[\sum_{k=1}^{\infty} \frac{(\sqrt{\rho'_i\rho_i})^{2k-1}}{2k-1} \right] \rho'_i \\ &= \frac{1}{\sqrt{\rho'_i\rho_i}} \left[\frac{1}{2} \log \left(\frac{1 + \sqrt{\rho'_i\rho_i}}{1 - \sqrt{\rho'_i\rho_i}} \right) \right] \rho'_i = \frac{1}{\sqrt{\rho'_i\rho_i}} \left[\text{artanh}(\sqrt{\rho'_i\rho_i}) \right] \rho'_i, \end{aligned}$$

which proves the expression for τ_i (4).

Next, we observed that $\tau'_i\tau_i = \text{artanh}^2(\sqrt{\rho'_i\rho_i})$ such that $\sqrt{\tau'_i\tau_i} = \text{artanh}(\sqrt{\rho'_i\rho_i})$ is the Fisher transformation of $\sqrt{\rho'_i\rho_i}$, which has inverse

$$\sqrt{\rho'_i\rho_i} = \tanh(\sqrt{\tau'_i\tau_i}) = \frac{e^{2\sqrt{\tau'_i\tau_i}} - 1}{e^{2\sqrt{\tau'_i\tau_i}} + 1}.$$

So, we can rewrite the expression $\tau_i = \frac{1}{\sqrt{\rho'_i\rho_i}} \sqrt{\tau'_i\tau_i} \rho_i$. which proves the expression for the

inverse mapping,

$$\rho_i = \sqrt{\frac{\rho'_i \rho_i}{\tau'_i \tau_i}} \times \tau_i = \frac{\tanh(\sqrt{\tau'_i \tau_i})}{\sqrt{\tau'_i \tau_i}} \times \tau_i.$$

The corresponding Jacobian is given by

$$\begin{aligned} \frac{\partial \rho_i}{\partial \tau'_i} &= \sqrt{\frac{\rho'_i \rho_i}{\tau'_i \tau_i}} I_r + \frac{(1 - \rho'_i \rho_i) \sqrt{\tau'_i \tau_i} - \sqrt{\rho'_i \rho_i}}{\tau'_i \tau_i} (\tau'_i \tau_i)^{-1/2} \tau_i \tau'_i \\ &= \sqrt{\frac{\rho'_i \rho_i}{\tau'_i \tau_i}} (I_r - P_{\tau_i}) + (1 - \rho'_i \rho_i) P_{\tau_i}, \end{aligned}$$

where we used that $\partial \sqrt{\rho'_i \rho_i} / \partial \sqrt{\tau'_i \tau_i} = \partial \tanh(\sqrt{\tau'_i \tau_i}) / \partial \sqrt{\tau'_i \tau_i} = 1 - \tanh^2(\sqrt{\tau'_i \tau_i}) = 1 - \rho'_i \rho_i$. \square

Proof of Theorem 2

We know that $Z|U \sim \text{CT}_{m,\nu}^{\text{std}}(\mu, \Xi)$ where $\mu = \boldsymbol{\rho}'U$ and $\Xi = \Lambda_\omega C_e^{1/2}$. We have the form of the score ∇_μ and $\nabla_\Xi = \nabla_{\text{vec}(\Xi)}$, such that

$$\nabla_\xi = \Theta' \begin{pmatrix} \nabla_\mu \\ \nabla_\Xi \end{pmatrix}, \quad \mathcal{I}_\xi = \Theta' \begin{pmatrix} \mathcal{I}_\mu & 0 \\ 0 & \mathcal{I}_\Xi \end{pmatrix} \Theta,$$

where $\Theta = \frac{\partial \theta}{\partial \xi'}$ with $\theta = [\mu', \text{vec}(\Xi)]'$. And by defining

$$\tilde{\xi} \equiv \begin{pmatrix} \mu \\ \sigma \\ \eta \end{pmatrix} = \begin{bmatrix} K_{2n} & \mathbf{0} \\ \mathbf{0} & I_{n(n-1)/2} \end{bmatrix} \xi \quad \text{where} \quad \xi = \begin{pmatrix} \text{vec}(\mu, \sigma)' \\ \eta \end{pmatrix},$$

where K_{2n} is the communication matrix, and we now have

$$\Theta = \frac{\partial \theta}{\partial \xi'} = \frac{\partial \theta}{\partial \tilde{\xi}'} \frac{\partial \tilde{\xi}}{\partial \xi'} = \begin{bmatrix} I_n & \mathbf{0} & \mathbf{0} \\ \mathbf{0} & \frac{\partial \text{vec}(\Xi)}{\partial \sigma'} & \frac{\partial \text{vec}(\Xi)}{\partial \eta'} \end{bmatrix} \begin{bmatrix} K_{2n} & \mathbf{0} \\ \mathbf{0} & I_{n(n-1)/2} \end{bmatrix},$$

where

$$\frac{\partial \text{vec}(\Xi)}{\partial \sigma'} = \frac{\partial \text{vec}(\Lambda_\omega C_e^{1/2})}{\partial \text{vec}(\Lambda_\omega)'} \frac{\partial \text{vec}(\Lambda_\omega)}{\partial \text{diag}(\Lambda_\omega)'} = (C_e^{1/2} \otimes I_n) E'_d,$$

and

$$\frac{\partial \text{vec}(\Xi)}{\partial \eta'} = \frac{\partial \text{vec}(\Lambda_\rho C_e^{1/2})}{\partial \text{vec}(C_e^{1/2})'} \frac{\partial \text{vec}(C_e^{1/2})}{\partial \text{vec}(C_e)'} \frac{\partial \text{vec}(C_e^{1/2})}{\partial \gamma'} B = (I_n \otimes \Lambda_\omega) (C_e^{1/2} \oplus I_n)^{-1} \frac{\partial \text{vec}(C_e^{1/2})}{\partial \gamma'} B,$$

and from Archakov and Hansen (2021, Proposition 3), we have

$$\frac{\partial \text{vec}(C_e^{1/2})}{\partial \gamma'} = (E_l + E_u)' E_l \left(I - \Gamma E_d' (E_d \Gamma E_d')^{-1} E_d \right) \Gamma (E_l + E_u)',$$

which uses the fact that $\partial \text{vec}(C)/\partial \text{vecl}(C) = E_l + E_u$, where E_l, E_u, E_d are elimination matrices, and the expression $\Gamma = \partial \text{vec}(C)/\partial \text{vec}(\log C)'$ is given in Linton and McCrorie (1995).

As for the matrix M , we have

$$M = \frac{\partial \text{vec}(\mu, \sigma)'}{\partial [\text{vec}(\mu, \sigma)]'} \frac{\partial \text{vec}(\mu, \sigma)}{\partial \tau'} = K_{n2} \begin{bmatrix} \frac{\partial \mu}{\partial \tau'} \\ \frac{\partial \sigma}{\partial \tau'} \end{bmatrix}$$

with $\boldsymbol{\tau} = (\tau_1, \tau_2, \dots, \tau_n) \in \mathbb{R}^{r \times n}$ and $\tau = \text{vec}(\boldsymbol{\tau})$, where

$$\begin{aligned} \frac{\partial \mu}{\partial \tau'} &= \frac{\partial \mu}{\partial \text{vec}(\boldsymbol{\rho}')'} \frac{\partial \text{vec}(\boldsymbol{\rho}')}{\partial \text{vec}(\boldsymbol{\tau}')'} \frac{\partial \text{vec}(\boldsymbol{\tau}')}{\partial \tau'}, \\ \frac{\partial \mu}{\partial \text{vec}(\boldsymbol{\rho}')'} &= \frac{\partial \text{vec}(\boldsymbol{\rho}' U)}{\partial \text{vec}(\boldsymbol{\rho}')'} = (U' \otimes I_n) \\ \frac{\partial \text{vec}(\boldsymbol{\rho}')}{\partial \text{vec}(\boldsymbol{\tau}')'} &= \sum_{i=1}^n \frac{\partial (I_d \otimes P_i) \rho_i}{\partial [(I_d \otimes P_i) \tau_i]'} = \sum_{i=1}^n (I_d \otimes P_i) J_i (I_d \otimes P_i'), \quad J_i = \frac{\partial \rho_i}{\partial \tau_i'} \\ \frac{\partial \text{vec}(\boldsymbol{\rho}')}{\partial \tau'} &= \sum_{i=1}^n (I_d \otimes P_i) J_i (I_d \otimes P_i') K_{dn} = \sum_{i=1}^n (I_d \otimes P_i) J_i (P_i' \otimes I_d) \\ \frac{\partial \mu}{\partial \tau'} &= (U' \otimes I_n) \sum_{i=1}^n (I_d \otimes P_i) J_i (P_i' \otimes I_d) \end{aligned}$$

where P_i is the i -th column of identity matrix I_n . Now using

$$\frac{\partial \text{diag}(\Lambda_\omega)}{\partial \text{vec}(\boldsymbol{\rho}')'} = \frac{\partial \text{diag}(\Lambda_\omega)}{\partial \text{diag}(\Lambda_\omega^2)'} \frac{\partial \text{diag}(\Lambda_\omega^2)}{\partial \text{diag}(\boldsymbol{\rho}' \boldsymbol{\rho}')'} \frac{\partial \text{diag}(\boldsymbol{\rho}' \boldsymbol{\rho}')}{\partial \text{vec}(\boldsymbol{\rho}' \boldsymbol{\rho}')'} \frac{\partial \text{vec}(\boldsymbol{\rho}' \boldsymbol{\rho}')}{\partial \text{vec}(\boldsymbol{\rho}')'} = -\frac{1}{2} \Lambda_\omega^{-1} E_d (I_{n^2} + K_n) (\boldsymbol{\rho}' \otimes I_n),$$

where $\text{diag}(\Lambda_\omega^2) = \iota_n - \text{diag}(\boldsymbol{\rho}' \boldsymbol{\rho}')$, we find

$$\begin{aligned} \frac{\partial \sigma}{\partial \tau'} &= \frac{\partial \text{diag}(\Lambda_\omega)}{\partial \tau'} = -\frac{1}{2} \Lambda_\omega^{-1} E_d (I_{n^2} + K_n) (\boldsymbol{\rho}' \otimes I_n) \frac{\partial \text{vec}(\boldsymbol{\rho}')}{\partial \tau'} \\ &= -\frac{1}{2} \Lambda_\omega^{-1} E_d (I_{n^2} + K_n) (\boldsymbol{\rho}' \otimes I_n) \sum_{i=1}^n (I_d \otimes P_i) J_i (P_i' \otimes I_d). \end{aligned}$$

This completes the proof of Theorem 2.

Proof of Theorem 3

Define $\mu_i = \rho_i' U$, $\sigma_i = \sqrt{1 - \rho_i' \rho_i}$, and the log-likelihood function is given by

$$\ell(Z_i|U) = c_v - \log(\omega_i) - \frac{\nu_i^* + 1}{2} \log\left(1 + \frac{e_i^2}{\nu_i^* - 2}\right)$$

where the interested parameter is τ_i . We have

$$\nabla_{\mu_i} = \frac{\partial(Z_i|U)}{\partial \mu_i}, \quad \nabla_{\omega_i} = \frac{\partial(Z_i|U)}{\partial \omega_i}, \quad \mathbb{E}[\nabla_{\mu_i \omega_i}] = 0,$$

and by defining $W_i = (\nu_i^* + 1)/(\nu_i^* - 2 + e_i^2)$, we have

$$\begin{aligned} \nabla_{\mu_i} &= W_i \frac{e_i}{\sigma_i} \\ \nabla_{\omega_i} &= W_i \frac{e_i^2}{\omega_i} - \frac{1}{\omega_i} \\ \mathcal{I}_{\mu_i} &= \mathbb{E}\left(W_i^2 e_i^2 / \omega_i^2\right) = \frac{(\nu_i^* + 1)\nu_i^*}{(\nu_i^* + 3)(\nu_i^* - 2)} \frac{1}{\omega_i^2} \\ \mathcal{I}_{\omega_i} &= \frac{1}{\omega_i^2} \mathbb{E}\left[(W_i e_i^2 - 1)^2\right] = \frac{2\nu_i^*}{\nu_i^* + 3} \frac{1}{\omega_i^2}. \end{aligned}$$

We now have

$$M_i \equiv \begin{bmatrix} \frac{\partial \mu_i}{\partial \tau_i'} \\ \frac{\partial \omega_i}{\partial \tau_i'} \end{bmatrix} = \begin{bmatrix} U' J_i \\ -\frac{1}{\omega_i} \rho_i' J_i \end{bmatrix} = \begin{bmatrix} U' \\ -\frac{1}{\omega_i} \rho_i' \end{bmatrix} J_i,$$

where we used that

$$\begin{aligned} \frac{\partial \mu}{\partial \tau_i'} &= \frac{\partial \mu}{\partial \rho_i'} \frac{\partial \rho_i}{\partial \tau_i'} = U' J_i \\ \frac{\partial \sigma_i}{\partial \tau_i'} &= \frac{\partial \omega_i}{\partial \omega_i^2} \frac{\partial \omega_i^2}{\partial (\rho_i' \rho_i)} \frac{\partial (\rho_i' \rho_i)}{\partial \rho_i'} \frac{\partial \rho_i}{\partial \tau_i'} = -\frac{1}{2\omega_i} (2\rho_i' J_i) = -\frac{1}{\omega_i} \rho_i' J_i = -\frac{\rho_i' J_i}{\sqrt{1 - \rho_i' \rho_i}}, \end{aligned}$$

and we arrive at the expressions

$$\nabla_{\tau_i} = M_i' \begin{pmatrix} \nabla_{\mu_i} \\ \nabla_{\omega_i} \end{pmatrix} = J_i \left[\frac{W_i e_i}{\omega_i} U - \frac{W_i e_i^2 - 1}{\omega_i^2} \rho_i \right],$$

and

$$\mathcal{I}_{\tau_i} = M_i' \begin{pmatrix} \mathcal{I}_{\mu_i} & 0 \\ 0 & \mathcal{I}_{\omega_i} \end{pmatrix} M_i = J_i \left[\frac{(\nu_i^* + 1)\nu_i^*}{(\nu_i^* + 3)(\nu_i^* - 2)} \frac{UU'}{\omega_i^2} + \frac{2\nu_i^*}{\nu_i^* + 3} \frac{1 - \omega_i^2}{\omega_i^4} \right] J_i.$$

We also have

$$\begin{aligned}
M_i^+ &= \frac{1}{U'U\rho'_i\rho_i - U'\rho_i\rho'_iU} J_i^{-1} \begin{bmatrix} U' \\ -\frac{1}{\omega_i}\rho'_i \end{bmatrix}' \begin{bmatrix} \rho'_i\rho_i & \omega_iU'\rho_i \\ \omega_iU'\rho_i & \omega_i^2U'U \end{bmatrix} \\
&= \frac{1}{U'U\rho'_i\rho_i - U'\rho_i\rho'_iU} J_i^{-1} \begin{bmatrix} U & -\frac{1}{\omega_i}\rho_i \end{bmatrix} \begin{bmatrix} \rho'_i\rho_i & \omega_iU'\rho_i \\ \omega_iU'\rho_i & \omega_i^2U'U \end{bmatrix} \\
&= \frac{1}{U'U\rho'_i\rho_i - U'\rho_i\rho'_iU} J_i^{-1} \begin{bmatrix} U\rho'_i\rho_i - \rho_iU'\rho_i & \omega_i(UU'\rho_i - \rho_iU'U) \end{bmatrix} \\
&= \frac{1}{U'U\rho'_i\rho_i - U'\rho_i\rho'_iU} J_i^{-1} \begin{bmatrix} \rho'_i\rho_iU' - \rho'_iU\rho'_i \\ \omega_i(\rho'UU' - U'U\rho'_i) \end{bmatrix}'.
\end{aligned}$$

This completes the proof of Theorem 3.

Proof of Theorem 4

For C a equicorrelation matrix with coefficient ϱ , we have $C = (1 - \varrho)I_n + \varrho\iota_n\iota'_n$,

$$C^{-1} = \frac{1}{1 - \varrho} \left(I_n - \frac{\varrho}{1 + (n - 1)\varrho} \iota_n\iota'_n \right),$$

and $|C| = [1 + (n - 1)\varrho](1 - \varrho)^{n-1}$. It follows that

$$X'C^{-1}X = \frac{X'X}{1 - \varrho} - \frac{\varrho X'\iota_n\iota'_n X}{(1 - \varrho)[1 + (n - 1)\varrho]},$$

such that

$$\begin{aligned}
\ell(X) &= c_\nu - \frac{1}{2} [\log(1 + (n - 1)\varrho) + (n - 1)\log(1 - \varrho)] \\
&\quad - \frac{\nu + n}{2} \log \left(1 + \frac{1}{\nu - 2} \left(\frac{X'X}{1 - \varrho} - \frac{\varrho X'\iota_n\iota'_n X}{(1 - \varrho)[1 + (n - 1)\varrho]} \right) \right).
\end{aligned}$$

Furthermore,

$$\frac{\partial \ell(X)}{\partial \varrho} = -\frac{1}{2} \left[\frac{(n - 1)}{1 + (n - 1)\varrho} - \frac{(n - 1)}{1 - \varrho} \right] - \frac{1}{2} W \left(\frac{X'X}{(1 - \varrho)^2} - \frac{[1 + (n - 1)\varrho^2] X'\iota_n\iota'_n X}{(1 - \varrho)^2 [1 + (n - 1)\varrho]^2} \right),$$

and from [Tong et al. \(2024, Theorem 3\)](#), we have

$$\begin{aligned}\mathcal{I}_A &= \frac{1}{4} \frac{(3\phi - 1)}{(1 + (n - 1)\varrho)^2} + \frac{\phi}{2} \frac{1}{(1 - \varrho)^2 (n - 1)} + \frac{1 - \phi}{4} \left[\frac{2}{(1 + (n - 1)\varrho)(1 - \varrho)} - \frac{1}{(1 - \varrho)^2} \right] \\ &= \frac{1}{4} \frac{(3\phi - 1)}{(1 + (n - 1)\varrho)^2} + \frac{\phi}{2} \frac{1}{(1 - \varrho)^2 (n - 1)} + \frac{1 - \phi}{4} \left[\frac{1 - (n + 1)\varrho}{(1 + (n - 1)\varrho)(1 - \varrho)^2} \right],\end{aligned}$$

such that

$$\mathcal{I}_\rho = \mathcal{I}_A (n - 1)^2 = \frac{1}{4} \frac{(3\phi - 1)(n - 1)^2}{(1 + (n - 1)\varrho)^2} + \frac{\phi(n - 1)}{2(1 - \varrho)^2} + \frac{1 - \phi}{4} \left[\frac{(1 - (n + 1)\varrho)(n - 1)^2}{(1 + (n - 1)\varrho)(1 - \varrho)^2} \right],$$

$\nabla_\eta = J\nabla_\varrho$ and $\mathcal{I}_\gamma = J^2\mathcal{I}_\varrho$, where $J = \frac{\partial\varrho}{\partial\gamma} = \frac{1}{(1 - \varrho)(1 + (n - 1)\varrho)}$. This completes the proof of [Theorem 4](#).

Proof of [Theorem 5](#)

For $e \sim \text{CT}_{n,\nu}^{\text{std}}(0, C^{1/2})$, where C is an equicorrelation matrix, we have

$$\begin{aligned}\ell(X) &= -\frac{1}{2} \log |C| + \sum_{i=1}^n c_i - \frac{\nu_i + 1}{2} \log \left(1 + \frac{1}{\nu_i - 2} V_i^2 \right) \\ &= -\frac{1}{2} [\log(1 + (n - 1)\varrho) + (n - 1) \log(1 - \varrho)] \\ &\quad - \sum_{i=1}^n \frac{\nu_i + 1}{2} \log \left(1 + \frac{1}{\nu_i - 2} V_i^2 \right),\end{aligned}$$

where $V = C^{-1/2}e$. We also have

$$C^{-1/2} = \frac{1}{\sqrt{1 - \varrho}} I_n + \left(\frac{1}{\sqrt{1 + (n - 1)\varrho}} - \frac{1}{\sqrt{1 - \varrho}} \right) \frac{1}{n} \mathbf{1}_n \mathbf{1}'_n,$$

such that

$$\begin{aligned}V_i &= \frac{1}{\sqrt{1 - \varrho}} e_i + \left(\frac{1}{\sqrt{1 + (n - 1)\varrho}} - \frac{1}{\sqrt{1 - \varrho}} \right) \bar{e} \\ &= \frac{1}{\sqrt{1 - \varrho}} (e_i - \bar{e}) + \frac{1}{\sqrt{1 + (n - 1)\varrho}} \bar{e}, \\ \frac{\partial V_i}{\partial \varrho} &= \frac{1}{2} \frac{1}{(1 - \varrho)^{3/2}} (e_i - \bar{e}) - \frac{1}{2} \frac{(n - 1)}{(1 + (n - 1)\varrho)^{3/2}} \bar{e}.\end{aligned}$$

The score is therefore given by

$$-2 \frac{\partial \ell(X)}{\partial \varrho} = \left[\frac{(n-1)}{1+(n-1)\varrho} - \frac{(n-1)}{1-\varrho} \right] + \sum_{i=1}^n W_i V_i \left[\frac{(e_i - \bar{e})}{(1-\rho)^{3/2}} - \frac{(n-1)\bar{e}}{(1+(n-1)\varrho)^{3/2}} \right].$$

We can use [Tong et al. \(2024, Theorem 5\)](#) to obtain the following expression for the information matrix,

$$\begin{aligned} \mathcal{I}_A &= \Omega_A (K_K + \Upsilon_K^e) \Omega_A + \frac{1}{4} E_d' \Xi E_d + \frac{1}{2} E_d' \Theta \Omega_A + \frac{1}{2} \Omega_A \Theta' E_d \\ &= \frac{1}{4} A^{-2} (1 + C_1) + \frac{1}{4} C_2 + \frac{1}{2} C_3 A^{-1}, \end{aligned}$$

where $A = 1 + (n-1)\rho$, and

$$\begin{aligned} C_1 &= n^{-1} (3\bar{\phi} - 2 - \bar{\psi}) + \bar{\psi}, \\ C_2 &= \delta^{-2} n^{-1} [3\bar{\phi} - 1 + (\bar{\psi} + 1)(n-1)^{-1}], \\ C_3 &= \delta^{-1} n^{-1} (\bar{\psi} + 2 - 3\bar{\phi}). \end{aligned}$$

The results now follows from $\mathcal{I}_\varrho = (n-1)^2 \mathcal{I}_A$, which completes the proof.

B Supplementary Material

Table B.1: Estimation of Marginal Volatility Models for Factors and Individual Stocks

Panel A: Factors						
	$a_0 (\times 10^{-4})$	a_1	b_0	b_1	b_2	b_3
MKT	4.554	-0.053	-0.219	0.968	-0.069	0.092
SMB	-0.556	-0.016	-0.151	0.983	-0.026	0.082
HML	-2.740	0.021	-0.120	0.992	-0.012	0.101
RMW	0.968	0.011	-0.084	0.993	0.014	0.056
CMA	-0.243	0.038	-0.087	0.993	0.006	0.060
UMD	2.764	0.083	-0.131	0.991	0.011	0.112
XLB	2.255	-0.015	-0.112	0.986	-0.049	0.063
XLE	2.482	-0.020	-0.116	0.987	-0.037	0.080
XLF	5.168	-0.038	-0.176	0.978	-0.055	0.106
XLI	3.381	-0.016	-0.156	0.978	-0.056	0.073
XLK	5.958	-0.052	-0.210	0.969	-0.056	0.093
XLP	3.478	-0.062	-0.236	0.966	-0.059	0.091
XLU	2.902	-0.026	-0.179	0.976	-0.027	0.091
XLV	4.105	-0.031	-0.244	0.961	-0.063	0.081
XLY	5.186	-0.022	-0.168	0.978	-0.046	0.090
Panel B: Individual Stocks						
	$a_0 (\times 10^{-4})$	a_1	b_0	b_1	b_2	b_3
Mean	4.227	-0.022	-0.124	0.980	-0.031	0.062
Q_5	0.084	-0.063	-0.287	0.950	-0.050	0.022
Q_{25}	2.712	-0.039	-0.150	0.976	-0.038	0.045
Q_{50}	3.996	-0.022	-0.110	0.984	-0.030	0.061
Q_{75}	5.625	-0.004	-0.075	0.989	-0.023	0.078
Q_{95}	8.896	0.022	-0.040	0.995	-0.011	0.102

Note: Panel A presents the estimation results of the AR(1)-EGARCH model for factors. Panel B shows the means and selected quantiles of the cross-sectional estimations for individual stocks in a large universe.

Table B.2: Stocks in Empirical Analysis

Subindustry	Symbols
Energy Sector (10)	
Oil & Gas Drilling	HP,NBR,RIG
Oil & Gas Equipment & Services	HAL,NOV,SLB
Integrated Oil & Gas	CVX,STO,XOM
Oil & Gas Exploration & Production	CNX,COG,EQT,RRR,SWN
Oil & Gas Storage & Transportation	FRO,OKE,WMB
Materials Sector (15)	
Fertilizers & Agricultural Chemicals	CF,FMC,MOS
Specialty Chemicals	ALB,ASH,CE,ECL,EMN,IFF,PPG,SHW
Metal, Glass & Plastic Containers	BLL,CCK,OI
Paper & Plastic Packaging Products & Materials	AVY,IP,MWV,PKG,SEE
Steel	ATI,CLF,NUE,STLD,TX,X
Industrials Sector (20)	
Aerospace & Defense	BA,GD,HRS,LMT,NOC,TDG,TXT,UTX
Building Products	AOS,BLDR,IR,MAS
Electrical Components & Equipment	AME,AYI,EMR,ENS,ETN,ROK
Construction Machinery & Heavy Trans. Equip.	CAT,CMI,MTW,PCAR,TEX,WAB
Industrial Machinery & Supplies & Components	DOV,FLS,IEX,ITT,ITW,PH,SNA,SWK,TKR
Trading Companies & Distributors	AIT,FAST,GWW,URI
Environmental & Facilities Services	ROL,RSG,SRCL
Human Resource & Employment Services	ADP,PAYX,RHI
Air Freight & Logistics	CHRW,EXPD,FDX,UPS
Rail Transportation	CSX,NSC,UNP
Cargo Ground Transportation	JBHT,ODFL,R
Consumer Discretionary Sector (25)	
Homebuilding	DHI,KBH,LEN,LEN,NVR,PHM
Leisure Products	BC,HAS,MAT
Apparel, Accessories & Luxury Goods	FOSL,HBI,PVH,RL,UA,VFC
Casinos & Gaming	LVS,MGM,PENN,WYNN
Hotels, Resorts & Cruise Lines	CCL,EXPE,MAR,RCL
Restaurants	CMG,DPZ,DRI,MCD,SBUX,YUM
Specialized Consumer Services	HRB,SCI,WTW
Broadline Retail	BIG,DDS,JWN,KSS
Apparel Retail	ANF,FL,GPS,ROST,TJX,URBN
Automotive Retail	AAP,AN,AZO,KMX,ORLY
Consumer Staples Sector (30)	
Consumer Staples Merchandise Retail	COST,DLTR,TGT,WMT
Packaged Foods & Meats	CAG,CPB,GIS,K,MKC,MKC,SJM
Household Products	CHD,CL,CLX,KMB,PG,

Note: Table continues on next page.

Table B.2: (cont.)

Subindustry	Symbols
Health Care Sector (35)	
Health Care Equipment	ABT,BAX,BDX,BSX,EW,MDT,SYK,TFX
Health Care Supplies	ALGN,COO,XRAY
Health Care Distributors	ABC,CAH,HSIC,MCK,PDCO
Health Care Services	CI,CVS,DGX,DVA,LH
Managed Health Care	CNC,HUM,MOH,UNH,WLP
Biotechnology	AMGN,BIIB,GILD,INCY,REGN,VRTX
Pharmaceuticals	BMY,LLY,MRK,NKTR,PFE,PRGO
Life Sciences Tools & Services	A,BIO,BIO,DHR,MTD,PKI,TECH,TMO,WAT
Financial Sector (40)	
Diversified Banks	CMA,FITB,KEY,PNC,USB,WFC
Regional Banks	BBT,FHN,HBAN,MTB,RF,SNV,ZION
Transaction & Payment Processing Services	FIS,FISV,GPN,JKHY,MA
Consumer Finance	ADS,AXP,COF,SLM
Asset Management & Custody Banks	AMG,BEN,BK,BLK,FII,NTRS,STT,TROW
Investment Banking & Brokerage	GS,MS,RJF,SCHW
Financial Exchanges & Data	CME,FDS,ICE,MKTX,NDAQ
Insurance Brokers	AJG,BRO,MMC
Life & Health Insurance	AFL,LNC,MET,PFM,PRU,TMK,UNM
Property & Casualty Insurance	ACGL,AIZ,ALL,CINF,HIG,PGR
Information Technology Sector (45)	
IT Consulting & Other Services	ACN,CTSH,IBM,IT,UIS
Application Software	ADBE,ADSK,ANSS,CDNS,CRM,INTU,SNPS,TYL
Systems Software	MSFT,ORCL,SYMC
Communications Equipment	CIEN,CSCO,FFIV,JNPR
Technology Hardware, Storage & Peripherals	AAPL,HPQ,NTAP,STX,WDC,XRX
Electronic Equipment & Instruments	CR,TDY,TRMB,ZBRA
Electronic Manufacturing Services	IPGP,JBL,SANM
Semiconductor Materials & Equipment	AMAT,KLAC,LRCX,TER
Semiconductors	ADI,AMD,INTC,MCHP,MPWR,MU,NVDA,SWKS,TXN
Utilities Sector (55)	
Electric Utilities	AEP,DUK,ETR,FE,LNT,PNW,PPL,SO,XEL
Multi-Utilities	AEE,CMS,CNP,DTE,ED,NI,SRE,WEC

Note: This table presents the symbols of the companies used in our empirical analysis, along with the names of their respective sectors and subindustries.